IMPACTS OF RESTORATION AND CLIMATE VARIABILITY ON PEATLAND GHG FLUXES

by

Marion Nyberg

B.SC., The University of Tasmania, 2018

A THESIS SUBMITTED IN PARTIAL FULFILLMENT OF

THE REQUIREMENTS FOR THE DEGREE OF

MASTER OF SCIENCE

in

THE FACULTY OF GRADUATE AND POSTDOCTORAL STUDIES

(Geography)

THE UNIVERSITY OF BRITISH COLUMBIA

(Vancouver)

August 2021

The following individuals certify that they have read, and recommend to the Faculty of Graduate and Postdoctoral Studies for acceptance, a thesis entitled:

Impacts of restoration and climate variability on peatland GHG fluxes

submitted by Marion Nyberg in partial fulfillment of the requirements for

the degree of Master of Science

in Geography

Examining Committee:

Dr. Sara Knox, Geography
Supervisor

Dr. T. Andrew Black, Land and Food Systems
Supervisory Committee Member

Dr. Mark Johnson, Institute for Resources, Environment and Sustainability
Supervisory Committee Member

Dr. Ian McKendry, Geography
Additional Examiner

Abstract

Peatland disturbance through drainage threatens to liberate large amounts of C stocks by increasing emissions of carbon dioxide (CO_2) from the soil. Restoration through re-wetting, on the other hand, could play an important role in climate change mitigation or adaptation by reducing CO_2 emissions and increasing the ability of peatland to sequester atmospheric CO_2. However, this can come at the cost of increased CH_4 emissions, an extremely potent greenhouse gas, and therefore rewetting can lead to a biogeochemical compromise between CO_2 uptake and storage, and CH_4 release. Currently, there is large uncertainty surrounding the extent of this compromise in ecosystems at different stages of recovery and with differing environmental conditions, making it difficult to predict how well these ecosystems are able to regain their function as CO_2 sinks following restoration. To assess the effect of re-wetting, I analysed eddy-covariance flux measurements alongside environmental variables from sites that have undergone different restoration techniques and consequently have different environmental conditions, mainly water table height (WTH). By the end of the one-year study period, the site with a higher water table, i.e., the wetter site, was a CO_2 sink, and the drier site was a CO_2 source. CH_4 emissions were higher at the wetter site annually and in the growing season, and whilst both sites had a positive radiative balance when calculated using sustained global warming potentials, the wetter site had a lower radiative balance on both a 20- and 100- year time horizon than the drier site, implying the importance of CO_2 sink status for climate benefits. These results emphasize the role that WTH and soil temperature have on promoting or inhibiting CO_2 and CH_4 emissions, and therefore can be used to inform management decisions and predict future trends in peatland ecosystems undergoing restoration.

Lay Summary

Peatlands are important ecosystems in the global carbon cycle as their soils are able to store vast quantities of carbon. However, when soils in peatlands are disturbed via drainage, they dry can release carbon dioxide (CO_2) into the atmosphere, thus contributing to global warming. Scientists have proposed re-wetting drained peatlands to reverse this effect and promote CO_2 uptake. This can be an issue, because wet conditions often lead to increased emissions of methane (CH_4), an extremely potent greenhouse gas. This study presents results comparing two peatlands undergoing restoration, one wetter, and one drier site, to determine the environmental conditions that maximise CO_2 uptake and minimize GHG emissions, thereby determining which conditions in restored peatlands are most beneficial for the climate.

Preface

With the assistance of the UBC Micrometeorology lab group, particularly Rick Ketler, I was responsible for maintaining and calibrating the field site instrumentation, as well as data analysis. The code to process the high frequency flux data was provided by my supervisor, Dr. Sara Knox and the R package, REddyProc (V2.2.0) by Thomas Wutzler. The code for gap filling methane using the random forest model was provided by Yeonuk Kim. NDVI data from satellite imagery was processed by Darian Ng. Data from "Delta-Burns Bog" was sourced from Environment Canada and Climate Change.

Table of Contents

List of Tables

List of Figures

List of Abbreviations and symbols

Abbreviation/symbol	Definition
α	Initial light response efficiency
AICc	Akaike Information Criterion corrected
ANCOVA	Analysis of covariance
C	Carbon
CH_4	Methane
CO_2	Carbon dioxide
EBC	Energy balance closure
FCH4	Methane flux
GHG	Greenhouse gas
GPP	Gross primary production
GPP_{max}	Maximum gross primary production when there are no light limitations
GWP	Global warming potential
H	Sensible heat flux
IRGA	Infrared gas analyser
LE	Latent heat flux
MDS	Multidimensional scaling
NEE	Net ecosystem exchange of CO_2
PAR	Photosynthetically active radiation
PARin	Incoming photosynthetically active radiation

RECO	Ecosystem respiration
RH	Relative humidity
SGWP	Sustained global warming potential
TA or T_a	Air temperature
tR	Magnitude of the water table amplitude
TS or T_s	5-cm soil temperature
uR	Estimated optimal water table position for CH_4 flux
WTH	Water table height

Acknowledgements

First and foremost, a huge thank you to my supervisor, Dr. Sara Knox, for offering seemingly endless time and help over the past two years. I've learnt so much from working with you and I'm grateful for all the assistance I've received and knowledge you've shared, despite how crazy the past couple of years have been. Global pandemic aside, I've had a wonderful grad school experience, and this is largely due to your supervision. I couldn't think of a better supervisor to move to the other side of the world to work with!

I'd also like to thank all of the Micrometeorology lab group for your help in the field and in lab. In particular, Rick Ketler for sharing so much technical knowledge of eddy covariance and meteorological equipment. I would've been lost without your patient explanations of how everything works, both in the lab and the bog! From long days setting up the eddy-covariance tower, to providing technical support over the phone when I've been out in the bog, I would've been lost without your help! Thanks to Sarah, Tin and Nick, for your continuous support and coming out to the bog to do field work with me, I really enjoyed spending time out there with you all and am grateful for the knowledge you've shared and the excellent company!

Thanks to the amazing staff in the geography department, particularly Danny, Sandy, Suzanne, Connie, Vincent and Julie, for your assistance on all things admin and technical, and making my grad school experience go a little smoother!

This study and the technical equipment was funded in part by Metro Vancouver, UBC (PI:Knox), the Canada Foundation for Innovation (Drs. Andreas Christen, Mark Johnson, Sara Knox), NSERC RTI (Dr. Andreas Christen), NSERC Discovery Grant (Knox). Financial support was providing through scholarships from the UBC Faculty of Graduate and Postdoctorate Studies and UBC Geography.

Dedication

This thesis is dedicated to the amazing friends I met during my time at UBC (particularly Emily, Gabby, Lauren and Sofie). There's no way I could've gotten through grad school, let alone a global pandemic, without you. Also, to my family back in Australia for always supporting me no matter where I move to, or what I pursue.

Chapter 1: Introduction

Peatlands are wetland ecosystems that in their natural state are not only large carbon (C) reservoirs, storing a vast proportion of global soil C (Roulet, 2000), but also providers of a multitude of other ecosystem services. To commodify the services provided by wetlands, the global value is estimated to be 26.4 trillion dollars per year; more than 20% of the total value of ecosystem services globally (Thorslund et al., 2017). Besides CO_2 sequestration this includes flood reduction, water filtration and wildlife habitat. Perhaps just as important, if not more so, is the significant cultural role peatlands play in many Indigenous cultures around the world (Schulz et al., 2019; Butler, C., 2019), a value often overlooked in the land and atmospheric sciences. Despite these values and services, at least 25% of peatlands globally have been disturbed through human activities such as land-use change, actions largely driven by economic growth (Page and Baird, 2016). However, as plants, animals and soils are removed and altered through these destructive activities, we observe shifts in ecosystem functioning and in particular, significant disruption to C and greenhouse gas (GHG) dynamics (Moreno-Mateos et al., 2012).

When disturbance occurs in peatlands it generally results in the shift from anaerobic to aerobic soil conditions (Abdalla et al., 2016), promoting decomposition of large soil C stores, and enhancing carbon dioxide (CO_2) emissions to the atmosphere (Fig. 1a & b). Drier soil also increases fire risk, which leads to substantial CO_2 emissions (Loisel et al., 2020). In response to increased CO_2 emissions from the soil, scientists and policymakers propose restoration efforts, e.g., rewetting drained peatlands, which enhances atmospheric CO_2 uptake and reduces CO_2 emissions (Tuittila et al., 1999). In terms of climate benefits, the key goals of peatland restoration include reinstating the C sink status, reducing GHG emissions, and returning the

environment to pre-disturbed conditions in terms of ecosystem functioning (Moreno-Mateos et al., 2012). Restoration therefore plays an important role as a natural climate solution, aiding in potential mitigation or adaptation to future change (Griscom et al., 2017). However, when rewetting peatlands, we must also consider the impact on the emission of methane (CH_4), a potent GHG with a global warming potential (GWP) 28-34 times that of CO_2 (Myhre, 2013). This is because many peatlands, both natural and restored, are sources of CH_4 to the atmosphere (Bridgham et al., 2013; Tan et al., 2019).

a

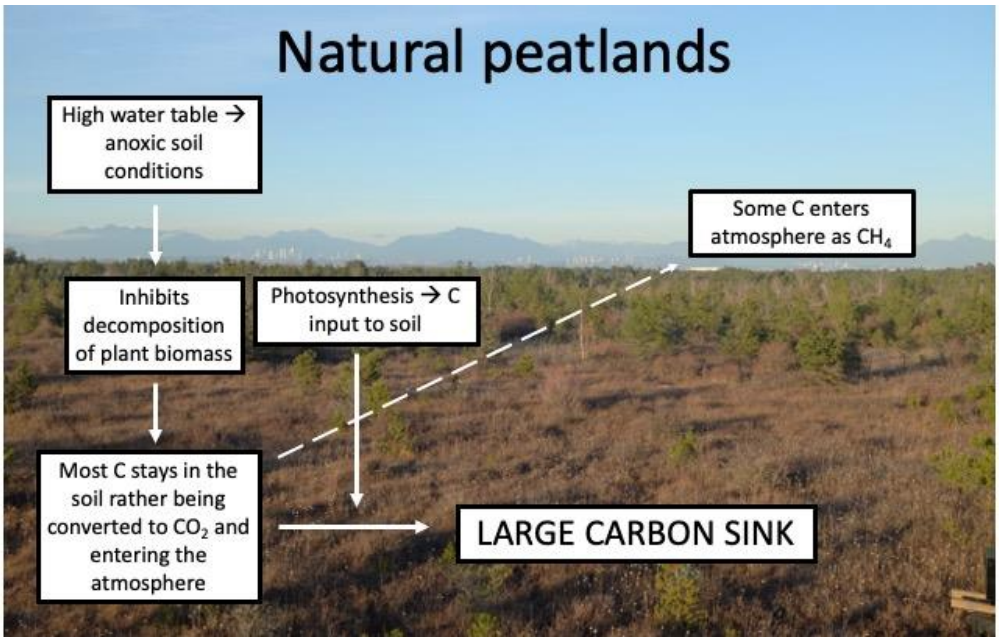

b

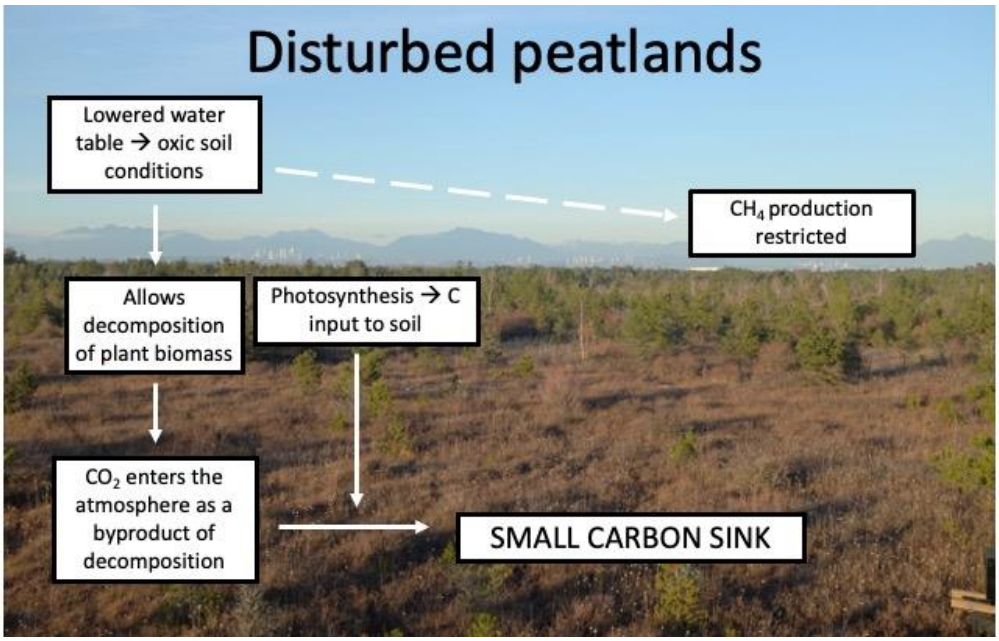

Figure 1. Simplified conceptual diagram of the effect of water table on carbon dioxide (CO_2) and methane (CH_4) dynamics in natural (a) and disturbed (b) peatlands.

Increased CH_4 emissions in peatlands undergoing restoration, compared to drained peatlands, is widely demonstrated (Petrescu et al. 2015) (Fig. 1a & b), and the large GWP potential associated

with CH_4 suggests a small increase could have serious implications for the climate (Yu et al., 2017). How CH_4 dynamics change over time in response to restoration and shifting environmental conditions is still largely unknown. When considering the climate impacts of GHGs, the rates of uptake and emission, as well as the difference in atmospheric lifetimes, particularly CH_4, relatively short-lived in the atmosphere, and CO_2, must be considered (Balcombe et al., 2018). CO_2 and CH_4 production and uptake depends on both biological and physical variables (Dean et al., 2018) that vary over a range of temporal scales (Hopple et al., 2020), and therefore it is likely that the C sink status and GHG emissions will depend on the stage the peatland is at in its recovery (Taillardat et al., 2020).

To understand how CO_2 enters and leaves the system (i.e., net ecosystem exchange [NEE]), we must recognise the main processes of CO_2 uptake and loss and consider some of the key drivers of C dynamics in peatland ecosystems. Uptake of atmospheric CO_2 via photosynthesis and subsequent input of C into plant biomass (i.e., gross primary production [GPP]), and release via ecosystem respiration (ER), both heterotrophic and autotrophic, are the two main processes that determine NEE. Whilst not an exhaustive list, many biophysical factors including water table height (WTH), soil temperature, vegetation type, and the interplay of these factors affect rates of GPP, ER, and consequently NEE, as they influence both plant and microbial functioning (Loisel et al., 2020). Changes in these factors therefore have the potential to influence the C sink or source status of an ecosystem (Knox et al., 2015; Petrescu et al., 2015). Thus, examining the response of CO_2 fluxes in peatlands to physical and biological factors can uncover important links and relationships which drive changes in C and GHG dynamics.

The predominant control of temperature on CO_2 fluxes is demonstrated widely in the literature (S.C. Lee et al., 2017; Strack and Zuback, 2013). Additionally, it has been established that there is an optimum temperature at which decomposing microbes work and respire CO_2 (Alster et al., 2020). When temperatures are too low respiration is inhibited, and increasing temperatures drive rates until they reach an optimum where we observe a plateau in the respiration rate (Carey et al., 2016). In peatland ecosystems, the temperature effect on CO_2 fluxes is modulated by WTH in that totally saturated soils suppress microbial activity, creating an anaerobic soil environment and limiting C losses via respiration (Davidson and Janssens, 2006). When the water table drops, creating aerobic soil conditions favored by some microbes, decomposition (and therefore respiration rates) increase (Beyer et al., 2021). Besides directly influencing NEE, WTH and temperature drive changes in plant species composition, affecting availability of C in the soil, i.e., substrate for microbes, and therefore rates of CO_2 uptake and release (Couwenberg et al., 2011; Lazcano et al., 2020).

Whilst the previous drivers of NEE have been physical properties of the ecosystem, the vegetation community represents an important biological control. As well as being responsible for autotrophic respiration, the vegetation community can alter the microbial respiration response to soil moisture and temperature though litter characteristics, and below ground mechanisms such as altered root activity and exudation (Almagro et al., 2009). Sphagnum mosses for example, which are common in many natural peatland ecosystems (Page and Baird, 2016), play a role in enhancing CO_2 uptake and promoting C storage (Nugent et al., 2018; Straková et al., 2010). However, shifts to an increase in vascular plant species, e.g. cotton grass (*Eriophorum vaginatum*), which can occur in response to a decreasing WTH, promotes soil microbial activity,

and thus greater losses of CO_2 from the soil due to enhanced availability of labile substrate (Dieleman et al., 2016; Gavazov et al., 2018). Despite promoting respiration, the presence of vascular plant species has also been linked to a larger C sink potential because they have higher rates of photosynthesis (Gavazov et al., 2018; Lazcano et al., 2020) suggesting the vegetation community plays an important role in mediating CO_2 fluxes.

It's well known that CO_2 is a large determinant of the C budget of an ecosystem, but for peatlands that are saturated for a large part of the year, CH_4 is also an important component of the C and GHG budgets, having a large effect on the global warming or cooling impact of peatland. Two microbial processes govern the production and oxidation of CH_4. Methanogenesis, performed by archaea in anoxic zones of the soil is the mineralisation of organic matter leading to the production of CH_4, and methanotrophy is the oxidation of CH_4 in aerobic conditions by bacteria that use CH_4 as their sole C and energy sources (Le Mer and Roger, 2001). Multiple pathways facilitate the transport of CH_4 through the soil to the atmosphere including ebullition (gas bubbles), via aerenchyma in vascular plants, diffusion in the soil or water column, or lateral movement across water ways as dissolved CH_4 (Dean et al., 2018). As expected, these mechanisms of CH_4 production and transport respond to a suite of physical and biological drivers.

As with NEE, temperature plays a dominant role in controlling CH_4 flux dynamics (Knox et al., 2015, 2016; Rinne et al., 2017). The temperature sensitivity of methanogenesis is higher than methanotrophy, so a small change in temperature can lead to large effects on CH_4 production (Le Mer and Roger, 2001). This is concerning considering the warming temperatures associated with

climate change and therefore the potential for positive feedback to the global climate-C cycle. However, the response of CH_4 dynamics to temperature is highly dependent on hydrology, as methanogenesis occurs in anaerobic environments (Dean et al., 2018). In fact, the role of WTH has been described to work much like an on or off switch, suppressing or promoting CH_4 release when the water table is around 10 cm above the soil surface (Christensen et al., 2013). Additionally, the WTH affects soil temperature by modulating the thermal properties of the soil, and therefore ecosystems with a higher WTH are likely to have a higher thermal diffusivity (van der Molen and Wijmstra, 1994), which will affect soil processes including methanogenesis. As described earlier, changes in WTH and temperature within an ecosystem can alter plant community composition, and therefore vegetation also plays an important role in mediating CH_4 fluxes.

The interplay of physical environmental factors and the vegetation community, which is one of the most significant drivers of CH_4 flux (Vanselow-Algan et al., 2015), can significantly alter production and release of CH_4. The combination of a high WTH and herbaceous vegetation with high root biomass and root exudates promotes methanogenesis through enhanced substrate availability (Lazcano et al., 2020; Waddington and Day, 2007). Additionally, the presence of vascular plants that contain aerenchymous tissue plays a role in facilitating the transport of CH_4 from where it is produced in anaerobic soil conditions, up to the atmosphere, thereby promoting emissions (Wilson et al., 2016a; Laanbroek, 2010). Conversely, oxidation of CH_4, can also occur as an effect of oxygen release from roots to the rhizosphere, (Laanbroek, 2010) and thus vascular plants play a key role in mediating CH_4 fluxes in peatland ecosystems.

Described above are the processes and key drivers that affect NEE and CH_4 exchange within natural peatlands. However, when these ecosystems are disturbed via draining for agriculture, peat harvesting, or urban development (Abdalla et al., 2016; Anderson et al., 2016; Wilson et al., 2016a), their functioning changes dramatically. Although land use change is associated with commodities such as peat for fuel, or food such as cranberries and rice, these commodities will eventually run out as farming can deplete organic matter (Bhatti and Tarnocai, 2009). Through land use change we lose invaluable ecosystem services, e. g. flood reduction, water filtration and potential for C sequestration (Page and Baird, 2016). Additionally, many peatlands have held spiritual significance for Indigenous communities and have traditionally been a place for harvesting, hunting and fishing (Schulz et al., 2019; Joosten, 2003; Burns Bog Overview, 2021). Unfortunately, with land use change we see the cultural values disregarded and diminished in society. In terms of GHG dynamics, whilst land use change can drive a decrease in CH_4 emissions where the peatland has been drained (Abdalla et al., 2016; Petrescu et al., 2015), this is usually accompanied by an increase in CO_2 emissions and a loss of soil C, as aerobic conditions promote ecosystem respiration (Beyer et al., 2021). When manipulation of the ecosystem via re-wetting occurs in order to dampen this response, we again see a shift in C and GHG dynamics.

Re-wetting can occur through an active process, e.g., ditch-blocking to raise the water table, or passively, e.g., through establishment of protected areas or being in close proximity to an actively re-wetted area. Generally following re-wetting, CH_4 emissions increase significantly (Strack and Waddington, 2012), and inundation duration post re-wetting plays a key role in influencing NEE (Zhao et al., 2019). Peatlands that are continuously inundated are likely to become a source of CH_4 to the atmosphere (Hemes et al., 2018), however, intermittent flooding

has led to significant decreases in CH_4 emissions (Altor and Mitsch, 2006, 2008; Whalen, 2010). WTH also plays a significant role in influencing the vegetation community. As the WTH can vary throughout ecosystem development, this means that plant species composition can change throughout the restoration process (Howie et al., 2009) and affect C and GHG dynamics. Unsurprisingly, the recovery of plant communities post restoration is not a fast process, and it is estimated that it takes on average 30 years to return to a pre-disturbed state (Moreno-Mateos et al., 2012). Thus, CO_2 and CH_4 dynamics in recently restored or recovering wetlands are likely to be substantially different to those in natural wetlands, with large interannual variations. It is also important to note that as re-wetting is often associated with increased CH_4 emissions, restoration often leads to a biogeochemical compromise between CO_2 and CH_4 emissions (Hemes et al., 2018; Petrescu et al., 2015). With peatland restoration being used as a natural climate solution, restoration management is vital, and by monitoring NEE and CH_4 fluxes alongside key variables that drive them within ecosystems undergoing different management, we can gain insight into whether we are meeting restoration goals and inform future management.

In communicating restoration progress or success and informing management decisions, we need to specify what we hope to achieve through restoration. Often there are both biodiversity and climate objectives such as animal habitat, flood reduction and the reinstatement of a C sink (Renou-Wilson et al., 2019; Wilson et al., 2009). Assessing and predicting how these factors will respond to restoration over time can be complicated, especially for C and GHG dynamics as they are controlled by variables such as vegetation and climate, which have large interannual variability (Couwenberg et al., 2011). Consistent monitoring of individual ecosystems is needed to assess restoration success as well as inform modelling efforts, as many current earth system

models have high uncertainty due to their coarse spatial resolution (Thorslund et al., 2017; Loisel et al., 2020). To communicate findings that have climate implications to other scientists, policy makers and land managers, global warming metrics such as the GWP, sustained global warming potential (SGWP) and radiative forcing (Neubauer and Megonigal, 2015) are used to indicate the relative radiative impacts of different GHGs (Neubauer, 2021). The time horizon over which predictions of C and GHG dynamics are made can affect the radiative balance of the ecosystem, and this, in combination with ecosystem development suggests that the climate effect of a recovering peatland will fluctuate over time (Page and Baird, 2016).

Evidently, the response of NEE and GHG fluxes to biophysical drivers is complicated, as many drivers, e.g., vegetation and hydrology, are inextricably linked, and vary over time. Changes in C storage over the long-term are slow, implying the need for more long-term studies to evaluate whether peatlands undergoing restoration are able to regain their C sink status, and match C storage values for natural peatlands (Moreno-Mateos et al., 2012; Yu et al., 2017). Whether or not the benefit of increased CO_2 sequestration and reduced emissions will outweigh the cost of CH_4 emissions in recovering peatlands in the long-term is still largely uncertain (Page and Baird, 2016). Enhancing our understanding of the drivers of GHG fluxes in peatlands undergoing restoration and with differing environmental conditions will be extremely beneficial for predicting future global C dynamics, improving management strategies to optimise C storage and minimize GHG emissions, and finally, to return them as close as possible to peatland ecosystems in a pre-disturbed state in terms of ecosystem function.

This thesis aimed to assess C and GHG ecosystem responses to disturbance and restoration by assessing continuous measurements of ecosystem-scale CO_2 and CH_4 fluxes as well as key environmental drivers in peatland sites with different environmental conditions. The study sites are located in the Burns Bog Ecological Conservancy Area (BBECA) in Metro Vancouver, B.C., Canada, which is a temperate raised bog ecosystem. Different areas of the BBECA have undergone a series of land-use changes including disturbance for agriculture and peat mining, and more recently, restoration via re-wetting. Hence, the BBECA is a highly heterogeneous environment with 24 ecosystem types that have been identified, mapped and described using terrestrial ecosystem mapping methodologies (Hebda et al., 2000). Prior to active restoration of the bog, abandonment and natural blockage of old ditches led to significant regeneration without any intervention. Considering the variation in historical disturbances and restoration strategies, GHG fluxes are likely to be quite variable throughout the bog. For this study I am comparing GHG fluxes at two sites representing two different dominant ecosystem types in the bog, which experienced different restoration strategies and consequently now differ in terms of vegetation type and water levels. This has important implications for future land management, as well as predicting peatland C cycle feedbacks. Specifically, I aimed to gain insight into how C and GHG dynamics vary in previously disturbed peatland ecosystems in the BBECA which have experienced different histories and restoration strategies, and consequently now differ in terms of vegetation type and WTH. My key questions were: 1.) How do C and GHG dynamics in the BBECA peatland vary with different environmental conditions? 2.) Which environmental conditions maximise C uptake whilst minimizing GHG emissions; and 3.) To what extent is enhanced CO_2 uptake offset by increased CH_4 emissions?

Chapter 2: Methods

2.1 Study area

2.1.1 First Nations acknowledgement

I would like to begin by acknowledging that my research takes place on the traditional, ancestral and unceded territory of the xʷməθkʷəy̓əm (Musqueam) people. I acknowledge, with gratitude and respect, that I am a guest on the lands and waters that the Musqueam people and their ancestors have called home since time immemorial.

2.1.2 Land use history

Traditionally, the land now named Burns Bog, was used by the Stó:lō, Katzie, Kwantlen, Semiahmoo, Tsawwassen and Musqueam First Nations for foraging, hunting and other cultural practices (Burns Bog Overview, 2021), but has since gone through multiple stages of land-use change. The Burns Bog Ecological Conservancy Area (BBECA) is a raised ombrotrophic bog located on the Fraser River Delta, on the west coast of BC, Canada. It was established in 2005 to conserve and restore the ecosystem functioning of this large coastal raised bog, which has undergone significant disturbance. Currently, the BBECA covers 2,363 hectares, however, this is only approximately half of the area historically occupied by the bog (Metro Vancouver, 2007). The substantial decrease in size is due to encroachment from agricultural and industrial land use, and the remaining bog area has undergone significant disturbance including peat mining, development, agriculture, and fire, leaving only approximately 29% of the bog undisturbed (Metro Vancouver, 2007). From the 1930s to the 1980s, peat extraction and cranberry farming was facilitated in the bog through establishment of drainage ditches directing the outward flow of water (Hebda et al., 2000). Drainage and subsequent drying of the bog increases peat

decomposition rates and promotes the establishment of larger, woody plants over bog-favouring species, mainly Sphagnum mosses. To this day, the bog's unique biodiversity and ecosystem functioning is under threat from nearby development and a rapidly changing climate. In response to these disturbances, since 2001, parts of the bog have undergone active restoration via ditch blocking to raise the water table in the hopes of promoting *Sphagnum* growth, conserving the unique ecological value of the bog, and reducing fire hazard. In others, natural regeneration has been occurring without human intervention. Consequently, areas of the bog are undergoing different management techniques and now differ in terms of vegetation type and water table levels (Hebda et al., 2000).

2.1.3 Measurement sites

To assess the impacts of restoration on C and GHG dynamics, two sites in the bog that have undergone different management and restoration approaches were chosen for the study (Fig. 2). These sites represent two different dominant ecosystem types in the bog. Both sites are equipped with eddy-covariance (EC) flux towers measuring GHG fluxes and meteorological variables. Based on climate normals and averages from Environment Canada from 1981-2010, the bog has an average annual temperature of 10.4ºC and annual rainfall of 1189 mm (Environment Canada, 2020).

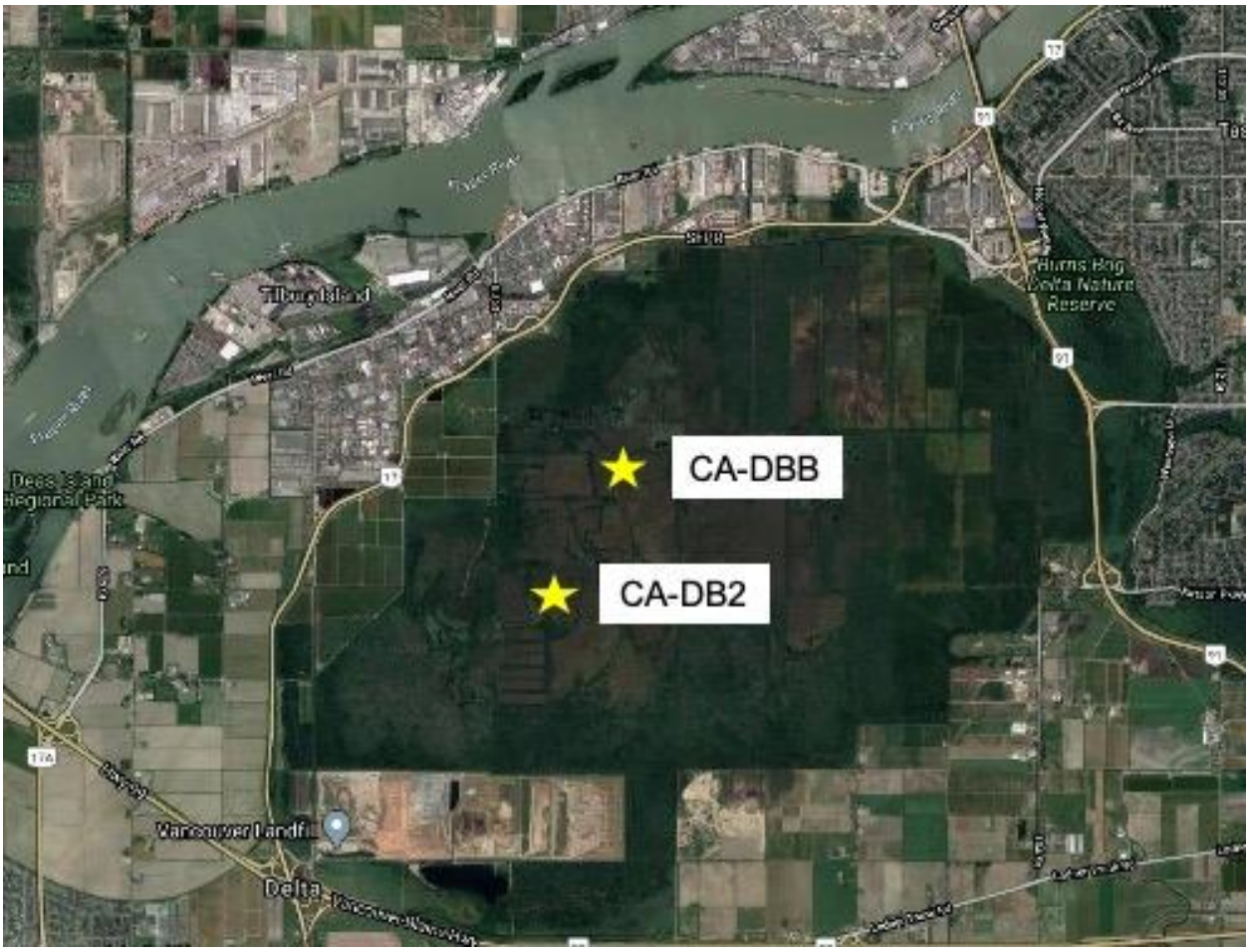

Figure 2. Map of Burns Bog Ecological Conservancy Area (BBECA) with stars indicating locations of study sites, CA-DBB and CA-DB2.

2.1.3.1 Burns Bog 1 (CA-DBB) "Actively rewetted site"

CA-DBB (49º07'45.49"N, 122º59'5.60"W) underwent peat harvesting between 1957 and 1963 using the Atkins-Durbrow hydropeat method (Heathwaite, 1993), and was rewetted in 2007 via ditch-blocking (Howie et al., 2009). The closest ditch to the tower, which is 70-m away, was blocked in 13 locations. During 2020, the water table height (WTH) ranged from -12.5 cm to 13.7 cm relative to the surface, and the annual mean WTH was 3.8 cm above the surface.

Throughout the year this site has areas of open water scattered throughout the landscape, likely an effect of active re-wetting. The peat depth is 5.8 m (Chestnutt, 2015) and the vegetation community is characterised by the sedge, white beak-rush (*Rhynchospora alba*), and *Sphagnum* mosses (Fig. 3a). The 90% average cumulative EC flux footprint at CA-DB2 was entirely inside the targeted area surrounding the tower during both the growing and non-growing season (Fig. 4a, c).

a b

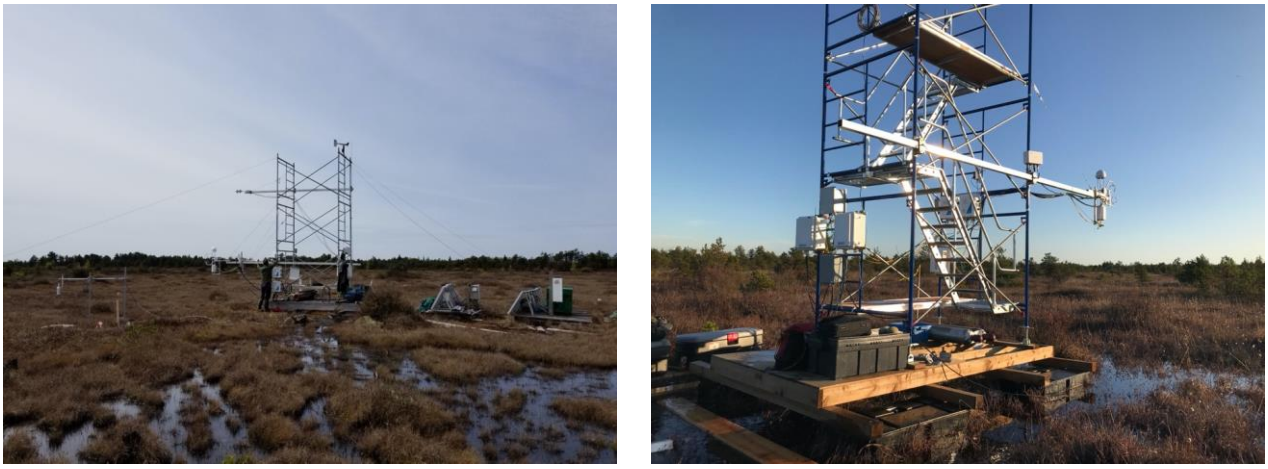

Figure 3. The EC flux towers at CA-DBB (a) and CA-DB2 (b). Photos taken by Sara Knox (2019/20)

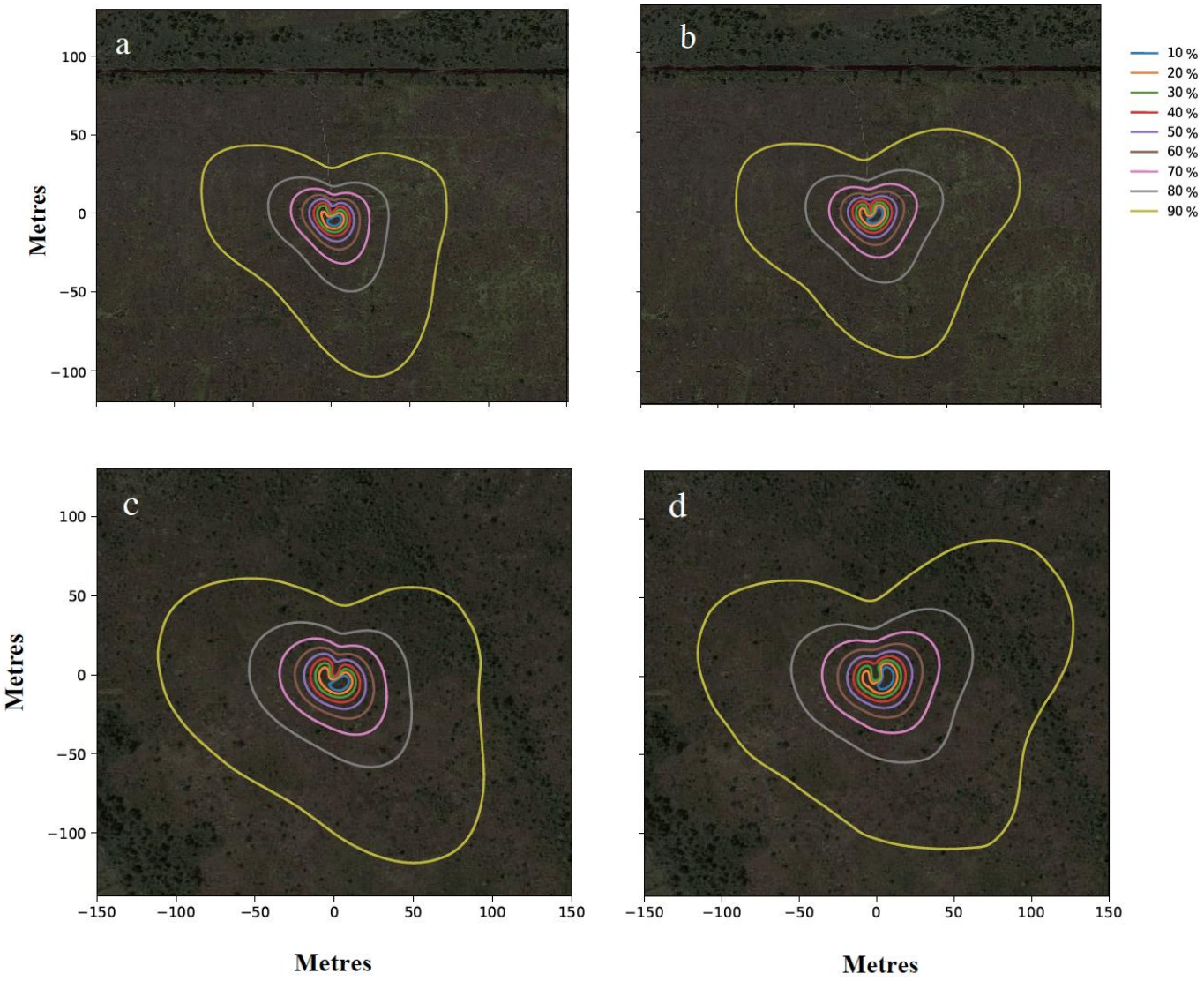

Figure 4. Flux footprint climatology contours during the study period for the growing season (a) and non-growing season at CA-DBB (c), and the growing season (b) and non-growing season at CA-DB2 (d).

2.1.3.2 Burns Bog 2 (CA-DB2) "Minimal re-wetted site"

CA-DB2 is approximately 1.5 km southwest of CA-DBB (49º07'8.33"N, 122º59'42.54"W) and underwent peat harvesting using the Atkins-Durbrow hydropeat method between 1930 and 1948. The closest ditch to the tower, which is 350-m away, was blocked in only 2 locations, and this, in

combination with the longer period of time it was abandoned after disturbance, drives an overall lower WTH and different vegetation composition to CA-DBB. Despite the lack of active rewetting, it is likely that active restoration at other locations in the bog has influenced water table dynamics, and additionally, beaver presence and dam creation has had the potential to create natural ditch blocking (Hebda et al., 2000). During 2020, WTH ranged from -39.9 cm to 16.5 cm relative to the surface. WTH at this site was overall lower than at CA-DBB, as indicated by the annual mean WTH of -2.7 cm. Peat depth at CA-DB2 is approximately 4 m (Briggs, 1976). The vegetation community is characterised by *Sphagnum* mosses and white beak-rush, as in CA-DBB, but there is also the presence of stunted lodgepole pine (*Pinus contorta*). This is a vegetation community resembling that of the original, undisturbed bog (Hebda et al., 2000) (Fig. 3b). The 90% average cumulative EC flux footprint at CA-DB2 was entirely inside the targeted area surrounding the tower during both the growing and non-growing season (Fig. 4b, d).

2.2 Meteorological and environmental measurements

Continuous meteorological and environmental variable measurements have been ongoing since 2014 at CA-DBB and October 2019 at CA-DB2. Sensors were positioned either directly on or within 10 m of the EC flux tower. Short and longwave radiation, both incoming and outgoing, were measured by a four-component net radiometer (CNR1, Kipp and Zonen, Delft, Holland) at the 4.25-m height at CA-DBB and 3.0-m height at CA-DB2. Incoming and outgoing photosynthetically active radiation (PAR) were measured by two quantum sensors (LI-190, LI-COR Inc., Lincoln, NE, USA) at the 1.8-m height at CA-DBB and 3.0-m height at CA-DB2. Precipitation was measured by an unheated tipping bucket rain gauge (TR-525 M, Texas Electronics, Dallas, Texas, USA) installed at the 1.0-m height within 10 m of both towers. Air

temperature (TA) and relative humidity (RH) were measured at the 2.0-m height on both towers (HMP 35-C, Vaisala Oy., Helsinki, Finland). Soil temperature (TS) was measured within 5 m of both towers over three replicate vertical profiles, which were then averaged, using thermocouples (Type T). Vertical profile depths at CA-DBB were -0.05, -0.1, -0.3, and -0.5 m, and at CA-DBB, +0.05, -0.05, -0.10, -0.3 m, with "+" indicating above the soil surface and "-" indicating below. WTH was measured using a pressure transducer (CS400, Campbell Scientific Inc. (CSI), Logan, UT, USA) relative to the soil surface, and soil volumetric water content (CS616, CSI) was measured at a depth of 0.30 m, both within 5 m of the tower at each site. Soil heat flux was measured using soil heat flux plates installed at 5-cm depth at three locations, which were then averaged, at each site. The 3 locations were approximately 30 cm apart in a hummock, hollow, and an intermediate location. Environmental variables were recorded every second at CA-DBB and every 10 seconds at CA-DB2, and 30-minute averages were computed. Some gaps in the data are expected due to energy constraints associated with solar power supply (i.e., cloudy periods throughout winter). In total, 3% and 7% of the meteorological data was missing from CA-DBB and CA-DB2, respectively.

2.3 Eddy-covariance measurements

The net exchange of CO_2 and CH_4 between the land surface and the atmosphere was estimated as 30-minute averages using the EC method. CO_2 flux measurements have been ongoing since 2014, and CH_4 fluxes (FCH4) since 2015 at CA-DBB, and both CO_2 and FCH4 since October 2019 at CA-DB2. Both sites have a similar set up and instrumentation, with the EC system installed at the 1.8-m height at CA-DBB and at the 2.5-m height at CA-DB2. Flux measurements are made using a sonic anemometer (CSAT-3, CSI), which measures wind velocity components

in the longitudinal, transverse and vertical wind directions and sonic temperature, an enclosed-path CO_2/H_2O infrared gas analyser (IRGA) (LI-7200, LI-COR Inc.), and an open-path gas analyser to measure the partial density of CH_4 (LI-7700, LI-COR Inc.). At both sites path separation was measured from the centre of the measurement instruments. At CA-DBB the northward path separation from the sonic anemometer for the LI-7700 is 0 cm, eastward separation is 15 cm, and the vertical separation is 0 cm. At CA-DB2, the northward separation is 29 cm, eastward separation 11 cm, and vertical separation 0 cm. At CA-DBB the northward separation of the sonic from the 7200 air sampling inlet funnel is 0 cm, eastward separation is 5 cm, and the vertical separation is 0 cm. At CA-DB2, the northward separation is 10 cm, eastward separation 0 cm and vertical separation 0 cm. The EC method measures the exchange of turbulent fluxes within the atmospheric surface layer, and thus allows an overview of flux exchange at the ecosystem scale (Burba, 2010). Specifically, it measures the covariance of the entity (e.g. CO_2 or CH_4) of interest and the vertical wind speed of circulating eddies. Both gas analysers are connected to an LI-7550 analyser unit (LI-COR inc.) equipped with a SMARTflux unit (Synchronization, Management, and Real Time Flux system, LI-COR inc.) Raw EC data measured at 20 Hz are processed using the EddyPro software v7.0.6 to obtain 30-minute averaged gas fluxes and related parameters. All fluxes are calculated by applying a double coordinate rotation method, spike removal, block averaging, and time-lag removal by covariance maximization (Moncrieff et al. 1997). Corrections were made for the effects of air density fluctuations on the half-hourly covariance of CO_2, CH_4, and H_2O fluxes (Webb et al. 1980). Both the LI-7200 and the LI-7700 mirrors were cleaned once the signal strength threshold for the LI-7700 reaches a value of 40 and were calibrated onsite every six weeks with a zero and span gas.

2.4 Filtering and gap-filling of CO_2 fluxes and FCH4

After calculating the fluxes, CO_2 and CH_4 flux values were filtered with low friction velocity (u_*) to constrain our analysis to turbulent conditions. Additionally, for the LI-7700, fluxes were filtered out that were less that 20% of the signal strength (LI-7700 Instruction manual, 2020). Using the R package REddyProc v 2.2.0, friction velocity thresholds (5%, 50% and 95% of 0.059 and 0.094 at CA-DBB and CA-DB2, respectively) were identified using a moving point test (Papale et al., 2006) and the data were then filtered for each threshold (Wutzler et al., 2018). Fluxes were further filtered for spikes in 30-minute mean densities, variances and covariances with thresholds varying between sites and quality checked using the flagging system proposed by Mauder and Foken (2006), where fluxes flagged as "2" were discarded from the dataset. Lastly, fluxes from wind directions outside the footprint of interest of each site were filtered from the data set and omitted from this analysis. For both sites, these were wind directions from 330° to 30°, to exclude wind passing through the tower from the north. After all QA/QC, missing CO_2 flux values were 42% and 34% at CA-DBB and CA-DB2, respectively, which includes data that were missing due to power limitations associated with inclement weather and low-light situations. Gaps in CO_2 and latent and sensible heat fluxes were filled using the marginal distribution sampling (MDS) method (Reichstein et al. 2005) with the REddyProc package (Wutzler et al. 2018). Net CO_2 fluxes were partitioned into gross primary production (GPP) and ecosystem respiration (RECO) using the night-time approach (Reichstein et al. 2005), also implemented in REddyProc (Wutzler et al. 2018). For CH_4, QA/QC resulted in missing CH_4 flux values of 55% and 47% at CA-DBB and CA-DB2, respectively, including missing data due to power limitations associated with inclement weather and low-light situations. There are as yet no

standards for gap-filling CH_4 flux measurements and this is an active and ongoing area of research (Nemitz et al. 2018). Gaps in CH_4 fluxes were filled using a random forest as described in Kim et al. (2020), as this approach was found to outperform MDS and other machine learning approaches (i.e., support vector machine and artificial neural networks).

2.5 Uncertainty estimation of CO_2 and FCH4

To estimate the uncertainty associated with the post-processing of fluxes, the REddyProc V.2.2.0 package was used (Wutzler et al. 2018). In this approach, bootstrapping of half-hourly EC measurements generates 200 artificial replicates of the dataset with different sized data gaps and a $u*$ threshold estimate for each. Subsequently, lower, median, and upper (5%, 50%, and 95% of the bootstrapping, respectively) estimates of $u*$ are determined and seasonal and annual NEE was calculated for each $u*$ threshold. Random uncertainty was also calculated, although it was not included in the total uncertainty due the values being negligible. NEE estimates were then partitioned to obtain RECO and GPP for each $u*$ threshold, and the error and uncertainties were estimated based on the confidence intervals (CIs) determined from the bootstrapping (Wutzler et al., 2018).

FCH4 uncertainty was estimated by generating 20 iterations of the gap filled timeseries and then calculating the standard deviation and 95% CI of the cumulative sums for the annual and seasonal time periods.

2.6 Energy balance closure

Energy balance closure (EBC) was calculated using daily (24-h) mean data as:

$$\mathrm{EBC} = (H + LE)/(R_n - G)$$

where *LE* is the latent heat flux, *H* is the sensible heat flux, R_n is net radiation and *G* is the soil heat flux. EBC was 79% and 96% at CA-DBB and CA-DB2, respectively.

2.7 Environmental effects on CO_2 and FCH4

The temperature sensitivity (Q10) of RECO and was estimated using using a linear fit between the logarithmic transformation of mean daily RECO (lnRECO) and soil temperature (*T*):

$$\mathrm{lnRECO} = A + bT$$

The temperature sensitivity of FCH4 was estimated using an exponential fit between mean daily FCH4 and *T*:

$$FCH4 = ae^{bT}$$

Where FCH4 is the measured mean daily lnFCH4, T is mean daily TS and a and b are parameters.

The Q10 values for CO_2 and CH_4 were then estimated as:

$$Q10CO2 = e^{10b}$$

$$Q10CH4 = e^{10b'}$$

The relationship between GPP and PAR was investigated using a rectangular hyperbolic light response curve derived from Michaelis-Menten kinetics (Frolking et al., 2006).

$$\mathrm{GPP} = \frac{\alpha \times \mathrm{PAR} \times \mathrm{GPP}_{max}}{\alpha \times \mathrm{PAR} + \mathrm{GPP}_{max}}$$

where α is the initial light response efficiency (μmol CO_2 (μmol photon)$^{-1}$), PAR is measured photosynthetically active radiation (μmol^{-1} m^{-2} s^{-1}), and GPP_{max} (μmol^{-1} m-2 s^{-1}) is the maximum gross primary production with no light restriction.

A nonlinear regression model was used to assess the response of CH_4 to WTH, following the equation by Turetsky et al., (2014):

$$FCH4 = FCH4\max \times \exp\left[0.5 \times \frac{(WTH - uR)^2}{(tR)^2}\right]$$

where FCH4 is the observed instantaneous CH_4 flux from EC measurements (mg CH_4 m^{-2} d^{-1}), $FCH4_{max}$ is the estimated maximum FCH4 at the optimal water position (mg CH_4 m^{-2} d^{-1}), WTH is expressed in cm, *uR* is the estimated optimal water table position for CH_4 flux (cm), and *tR* is an estimate of the magnitude of the WTH amplitude (cm) (Turetsky et al., 2014).

2.8 NDVI

Normalized difference vegetation index (NDVI), an indicator of plant greenness, was estimated from Landsat 8 satellite imagery obtained courtesy of the U.S. Geological Survey. The data were processed using Google Earth Engine, and NDVI was extracted from the pixels that fell within the flux footprint (Fig. 3). NDVI data were used to evaluate the photosynthetic capacity between sites and how it changes over the year. It is also compared alongside GPP to assess whether NDVI values were correlated with greater CO_2 uptake. Due to satellite image availability which varied between once every 1-3 weeks, gaps were filled using linear interpolation between dates.

2.9 Data analysis

All data were analysed using R (version 4.0.1). Analyses were made over annual timescales, and data was further divided into the growing and non-growing season, with differences between annual and seasonal cumulative CO_2 and CH_4 fluxes considered significant if there was no overlap in the 95% CIs and differences between environmental variables tested using the Kruskal-Wallis test and a significance level of $p < 0.05$. The growing season was determined as 1 April until 30 September and the non-growing season 1 October until 31 March. To investigate effects of environmental drivers on RECO, it was log transformed to better meet assumptions for normality for use in subsequent regression modelling. To investigate effects of environmental drivers on daily mean FCH4, it was transformed by first adding a constant of 8 mg CH_4 m^{-2} day^{-1} at CA-DBB and 20 mg CH_4 m^{-2} day^{-1} at CA-DB2 to allow values of near 0 emissions, and then log transformed to attain a normal distribution before further analysis (Olefeldt et al., 2013; Turetsky et al., 2014). To determine differences in environmental variables and daily mean CO_2 and CH_4 fluxes between sites, I used analysis of covariance (ANCOVA) and to investigate how environmental drivers affected CO_2 fluxes and FCH4, I used stepwise linear regression. To determine the GHG balance of the two sites I used sustained global warming potentials (SGWP) to assess the relative radiative impacts of CH_4 (Neubauer, 2021) over different time horizons. SGWPs of 45 and 96 were used for CH_4 on a 100- and 20- year timeline respectively (Neubauer and Megonigal, 2015) and values were calculated in units of g CO_2-eq m^{-2} yr^{-1}. The radiative balance was calculated as follows:

$$\text{Radiative balance} = \left((NEE - FCH4) \times \left(\frac{44.01}{12.01}\right)\right) + \left((FCH4 \times \left(\frac{16.04}{12.01}\right)) \times SGWP\right)$$

Where NEE is the cumulative annual NEE in g C m^{-2}, FCH4 is cumulative annual FCH4 in g C m^{-2}, SGWP is either 96 or 45 depending whether the radiative balance is being calculated on a 20- or 100- year time horizon, respectively.

Chapter 3: Results

3.1 Environmental variables

Air temperature (TA) ranged from -7.5 °C and -7.6 °C in January 2020 to 22.7 °C and 21.3 °C in August 2020 at CA-DBB and CA-DB2, respectively (Fig. 5a). TA at CA-DB2 was significantly lower ($p < 0.05$) than at CA-DBB throughout the study period, with average annual air temperatures being 1.1 °C lower. 10-year average annual climate data acquired from Environment Canada and Climate Change (ECCC) at the nearest weather station to the site ("Delta- Burns Bog") indicates that CA-DBB was 0.4 °C higher and CA-DB2 was 0.65 °C lower than the 10.2 °C 10-year annual average (Table 1). The two study sites differed from the 10-year average consistently throughout the year, with the largest above average temperatures in the non-growing season months from December to February (Fig. 5a).

Due to the close proximity of the study sites, precipitation (P) values were used from CA-DB2 to represent both sites. In 2020, total cumulative precipitation ranged from 395.5 mm in the growing season to 1099.9 mm in the non-growing season (Fig. 5b). 2020 experienced nearly a 20% higher cumulative annual rainfall than the ECCC 10-year average (Table 1). The largest difference in rainfall was during the non-growing season, when Burns Bog experienced 211.6 mm more rainfall than the ECCC 10-year average, with the majority of this falling in January (Fig. 5b). In the growing season, Burns Bog experienced 85.4 mm more precipitation than the ECCC average, with the largest difference in May (Fig. 5b).

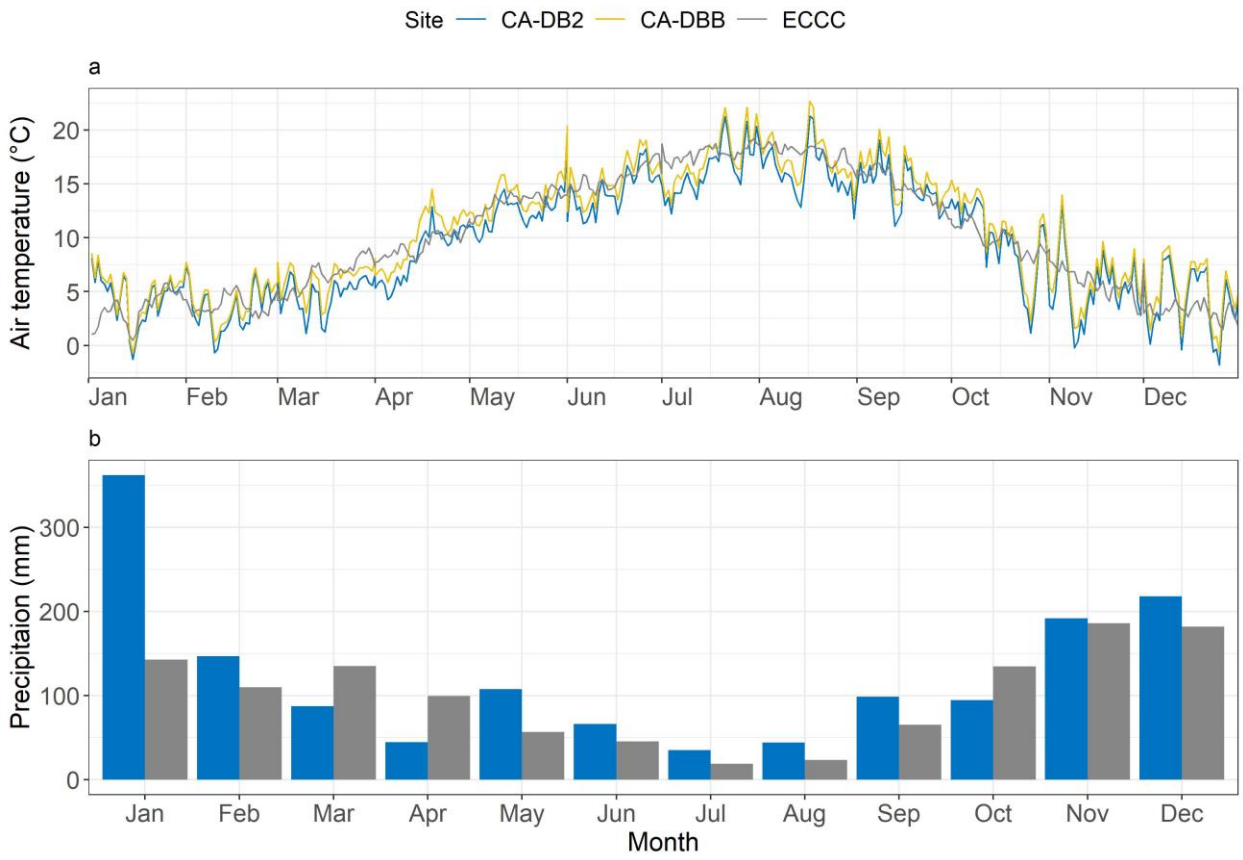

Figure 5. Daily mean air temperature (a) and cumulative monthly precipitation (b) over the duration of the study period in 2020 for CA-DB2, CA-DBB and the ECCC 10-year average.

Throughout the study period, soil temperature at the 5-cm depth (TS) ranged from 2.6 °C and 0.6 °C in January 2020 to 19 °C and 20.7 °C in July 2020 at CA-DBB and CA-DB2, respectively (Fig. 6a). As with TA, TS was significantly lower ($p < 0.05$) throughout the study period at CA-DB2, with the average annual temperature being 0.9 °C lower than at CA-DBB (Table 1).

WTH ranged from -12.5 cm to 13.7 cm at CA-DBB and -39.9 cm to 16.5 cm at CA-DB2 (Fig. 6b). On average it was below the soil surface during the growing season, and above the surface during the non-growing season for both sites (Table 1; Fig. 6b). The WTH range at CA-DBB

was just under half of that at CA-DB2, implying CA-DB2 has stronger seasonality in inundation than CA-DBB. Throughout the study period, WTH at CA-DB2 was significantly lower than CA-DBB ($p < 0.05$), being on average 6.5 cm lower annually, and up to 11.5 cm in the growing season. Whilst still significantly lower during the non-growing season, the difference was much less, being on average 2 cm lower at CA-DB2. Hence, the soil at CA-DB2 was overall drier than at CA-DBB.

Vapour pressure deficit (VPD) ranged from an average of 0.10 kPa during the non-growing season to 0.40 kPa during the growing season at both sites, and there was no significant difference in the annual average VPD between sites (Table 1; Fig 6c).

Figure 6. Daily mean 5-cm soil temperature (a), water table height (WTH) relative to the soil surface, and vapour pressure deficit (c) over the duration of the study period in 2020 for CA-DB2 and CA-DBB.

Mean NDVI was significantly lower ($p<0.05$) throughout the study at CA-DBB than CA-DB2 (Table 1; Fig. 7a). At CA-DB2, NDVI remained roughly the same throughout the year, being on average 0.5. At CA-DBB, NDVI increased significantly ($p < 0.05$) from 0.47 in the non-growing season to 0.53 in the growing season.

As the two sites are located only 1.5 km apart with little to no obstruction for incoming radiation, incoming photosynthetically active radiation (PARin) was used from CA-DB2 to represent both sites. Over the study period, total PARin ranged from 162.2 mol m^{-2} $month^{-1}$ in December to

1373.2 mol m^{-2} $month^{-1}$ in July (Fig. 7b). Total annual PARin was 9,166.2 mol m^{-2}, with 7,052.2 mol m^{-2} in the growing season and 2,177.6 mol m^{-2} in the non-growing season (Table 1).

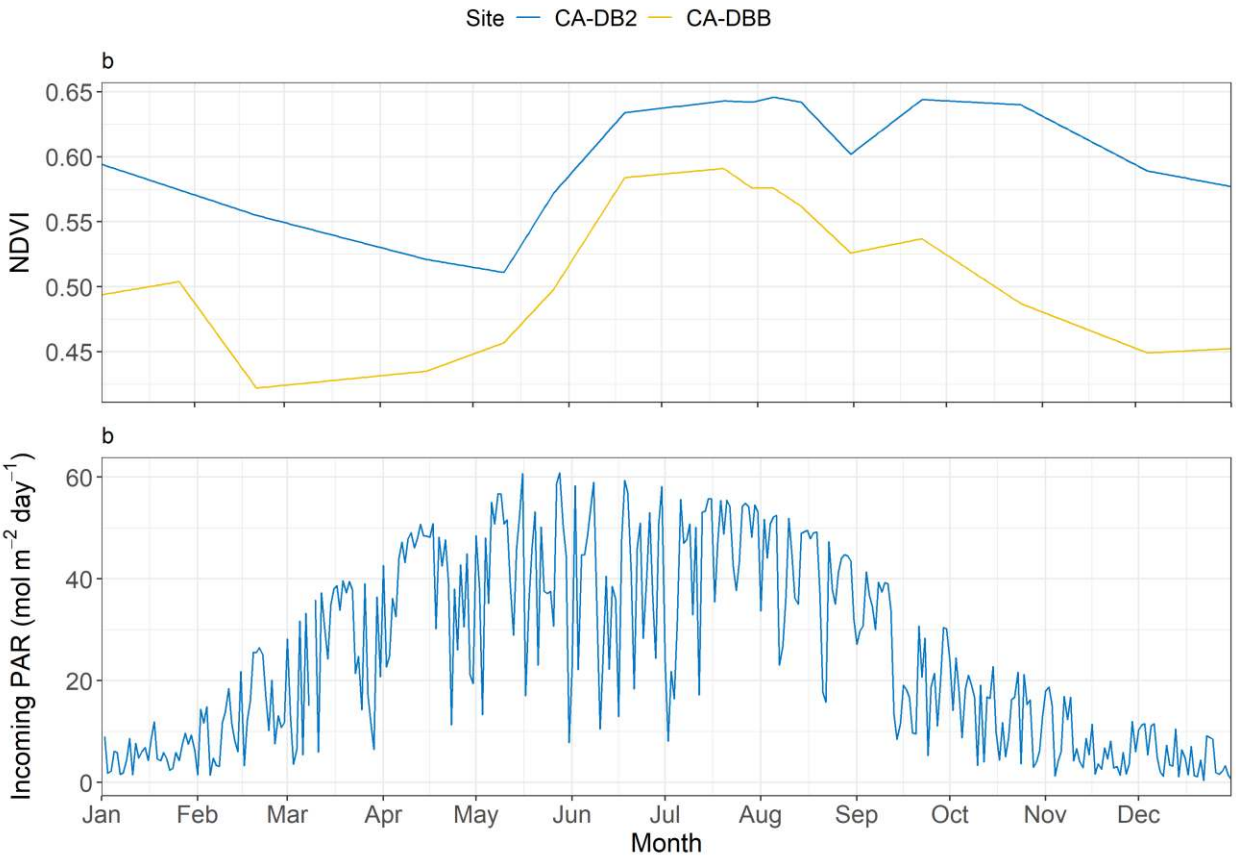

Figure 7. Normalized difference vegetation index (a) and daily mean incoming photosynthetically active radiation (b) over the duration of the study period in 2020 for CA-DB2

Table 1. Annual and seasonal mean, or cumulative environmental variables for the two sites and the 10-year Environment and Climate Change Canada average. * indicates statistically significant values (P < 0.05) between CA-DBB and CA-DB2. Values in brackets indicate difference from ECCC 10-year average.

Site	Annual	Growing season	Non-growing season
TA (℃)			
CA-DBB	10.6 (0.4)	15.1 (0.3)	6.1 (0.6)
CA-DB2	9.5* (-0.65)	13.8* (-1.0)	5.3* (-0.2)
ECCC 10-year	10.2	14.8	5.5
TS 5cm (℃)			
CA-DBB	11.5	15.8	7.3
CA-DB2	10.6*	15.4*	5.8*
Total cumulative precipitation (mm)			
CA-DB2	1495 (297)	396 (85)	1100 (212)
ECCC 10-year	1199	310	888
WTH (cm)			
CA-DBB	3.8	-0.4	8.1
CA-DB2	-2.7*	-11.5*	6.1*
VPD (kPa)			
CA-DBB	0.2	0.4	0.1
CA-DB2	0.3	0.4	0.1
PARin (mol m^{-2})			
CA-DB2	9229.8	7052.2	2177.6
NDVI			
CA-DBB	0.5	0.5	0.5
CA-DB2	0.6*	0.6*	0.59*

3.2 CO_2 fluxes

The two sites differed significantly in their cumulative annual NEE in 2020. CA-DBB was a CO_2 sink of 26.2 ± 16.1 g C-CO_2 m^{-2}, whereas CA-DB2 was a CO_2 source (27.4 ± 18.1 g C-CO_2 m^{-2}) (Table 2; Fig. 8a). Both sites were CO_2 sinks in the growing season and CO_2 sources in the non-growing season (Table 2; Fig. 8b). In the growing season, daily mean NEE was -0.4 g C-CO_2 m^{-2} and -0.2 g C-CO_2 m^{-2} at CA-DBB and CA-DB2 ($p = 0.01$), respectively, and the cumulative growing season sink strength at CA-DBB was over twice as strong (-74 ± 5.8 g C-CO_2 m^{-2}) than at CA-DB2 (-32.8 ± 4.6 g C-CO_2 m^{-2}) implying CA-DBB had higher CO_2 uptake during the growing season (Table 2). During the non-growing season, when both sites were net CO_2 sources to the atmosphere, daily mean NEE was 0.3 g C-CO_2 m^{-2} and 0.4 g C-CO_2 m^{-2} at CA-DBB and CA-DB2, respectively ($p < 0.05$). Consequently, in the non-growing season, CA-DB2 emitted 24% more CO_2 (60.2 ± 7.3 g C-CO_2 m^{-2}), than CA-DBB (48.7 ± 6.9 g C-CO_2 m^{-2}) (Table 2). At CA-DB2, the weaker CO_2 sink strength in the growing season, coupled with stronger source strength in the non-growing season led to CA-DB2 being a CO_2 source.

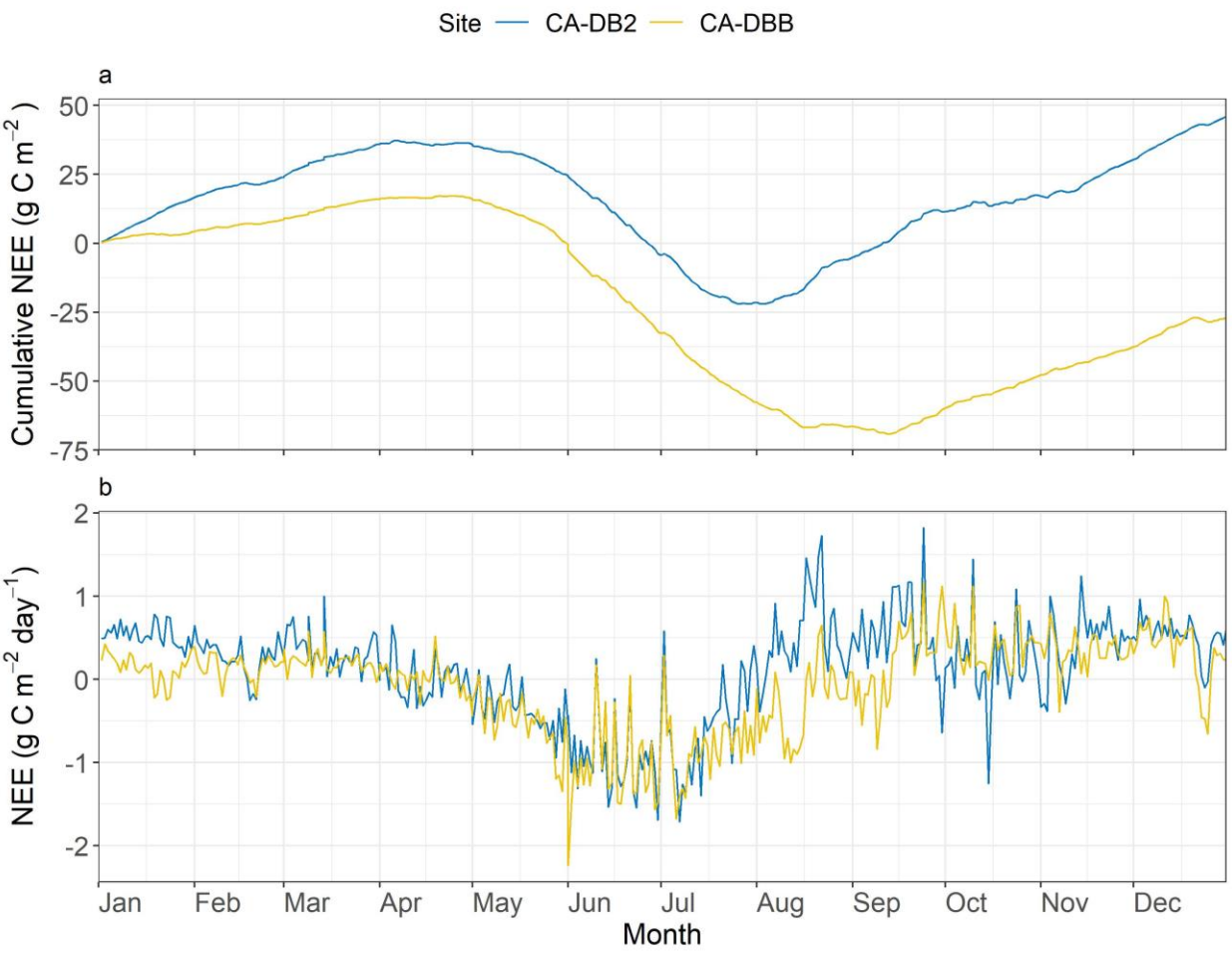

Figure 8. Cumulative net ecosystem exchange of CO_2 (NEE) (a) and daily NEE (b) over the duration of the study period in 2020 at CA-DB2 and CA-DBB.

When NEE is partitioned into its components, GPP and RECO, the drivers of the seasonal and annual differences in NEE between sites becomes clearer. Annual GPP was 34% higher at CA-DB2 (518.3 ± 11.1 g C-CO_2 m^{-2}) than CA-DBB (387.3 g ± 39.4 C-CO_2 m^{-2}) (Table 2; Fig. 9a), and this trend was similar in the growing and non-growing seasons. In the growing season, GPP at CA-DB2 was 438.8 ± 28.6 g C-CO_2 m^{-2}, which was 33% higher than CA-DBB, which was 329.6 ± 28.2 C-CO_2 m^{-2}. The difference between sites became even more prominent in the non-

growing season, with GPP 37% higher at CA-DB2 (79.5 ± 16.15 g C-CO_2 m^{-2}) than at CA-DBB (58.1 ± 51.6 g C-CO_2 m^{-2}) (Table 2; Fig. 9b). GPP peaked in June at CA-DBB (82.5 g C-CO_2 m^{-2} mon^{-1}) and in July at CA-DB2 (95 g C-CO_2 $m^{-2}mon^{-1}$) However, despite higher rates of GPP, CA-DB2 also had higher annual and seasonal RECO than CA-DBB, leading to RECO offsetting CO_2 uptake through GPP and thus resulting in CA-DB2 being a CO_2 source (Table 2; Fig. 10a). Specifically, annual RECO was 51% higher at CA-DB2 (545.6 ± 11.4 g C-CO_2 m^{-2}) than at CA-DBB (361.5 ± 44.5 g C-CO_2 m^{-2}) (Table 2). In the growing season, RECO was 59% higher at CA-DB2 (406 ± 27.6 g C-CO_2 m^{-2}) than at CA-DBB (255.7 ± 34 g C-CO_2 m^{-2}) and 32% higher in the non-growing season (139.6 ± 10.9 g C-CO_2 m^{-2} at CA-DB2 and 105.9 ± 56.9 g C-CO_2 m^{-2} at CA-DBB) (Table 2). Hence, CA-DB2 had higher RECO throughout the study period and there was a larger relative difference in RECO between sites in the growing season.

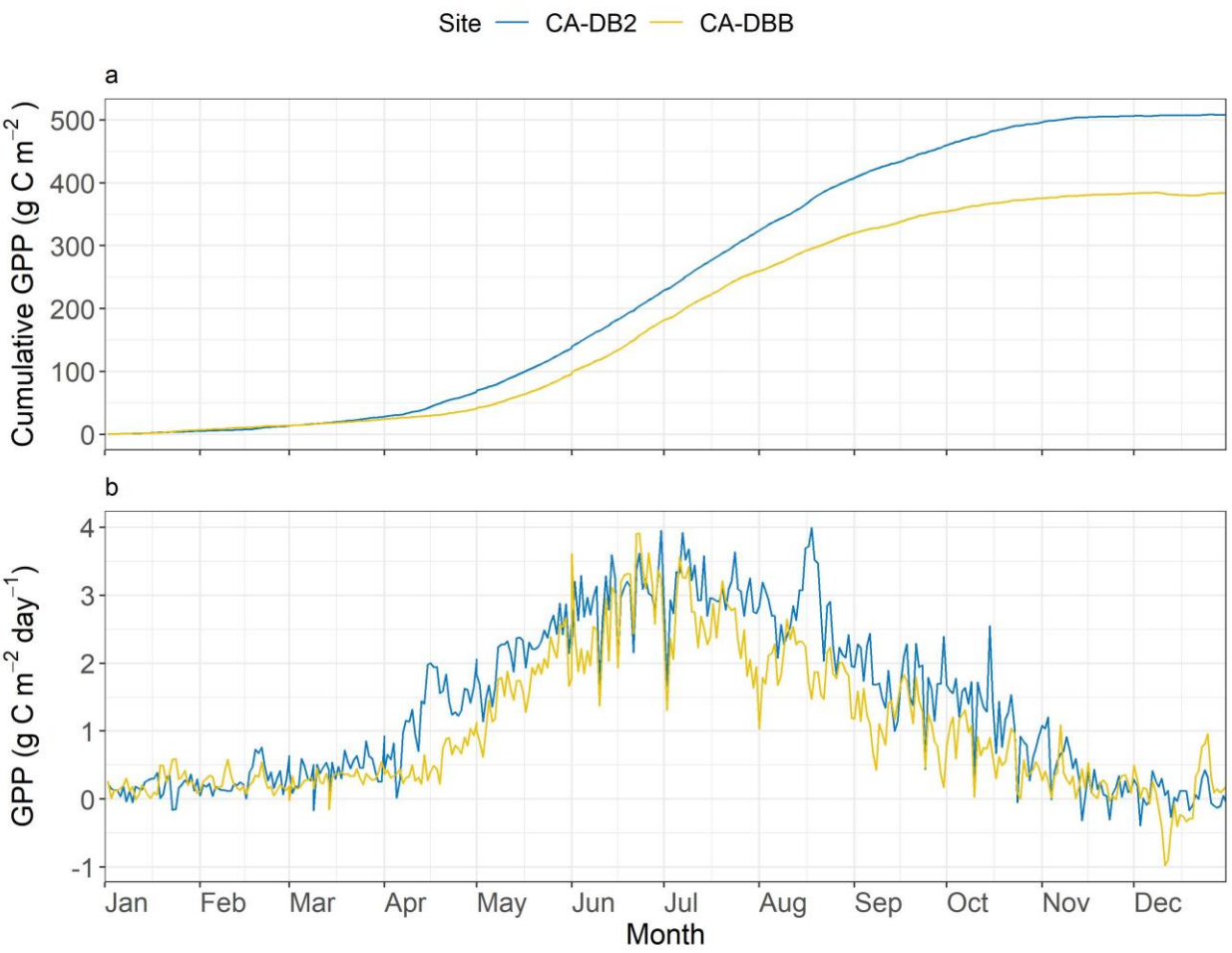

Figure 9. Cumulative gross primary productivity (GPP) (a) and daily GPP (b) over the duration of the study period in 2020 at CA-DB2 and CA-DBB.

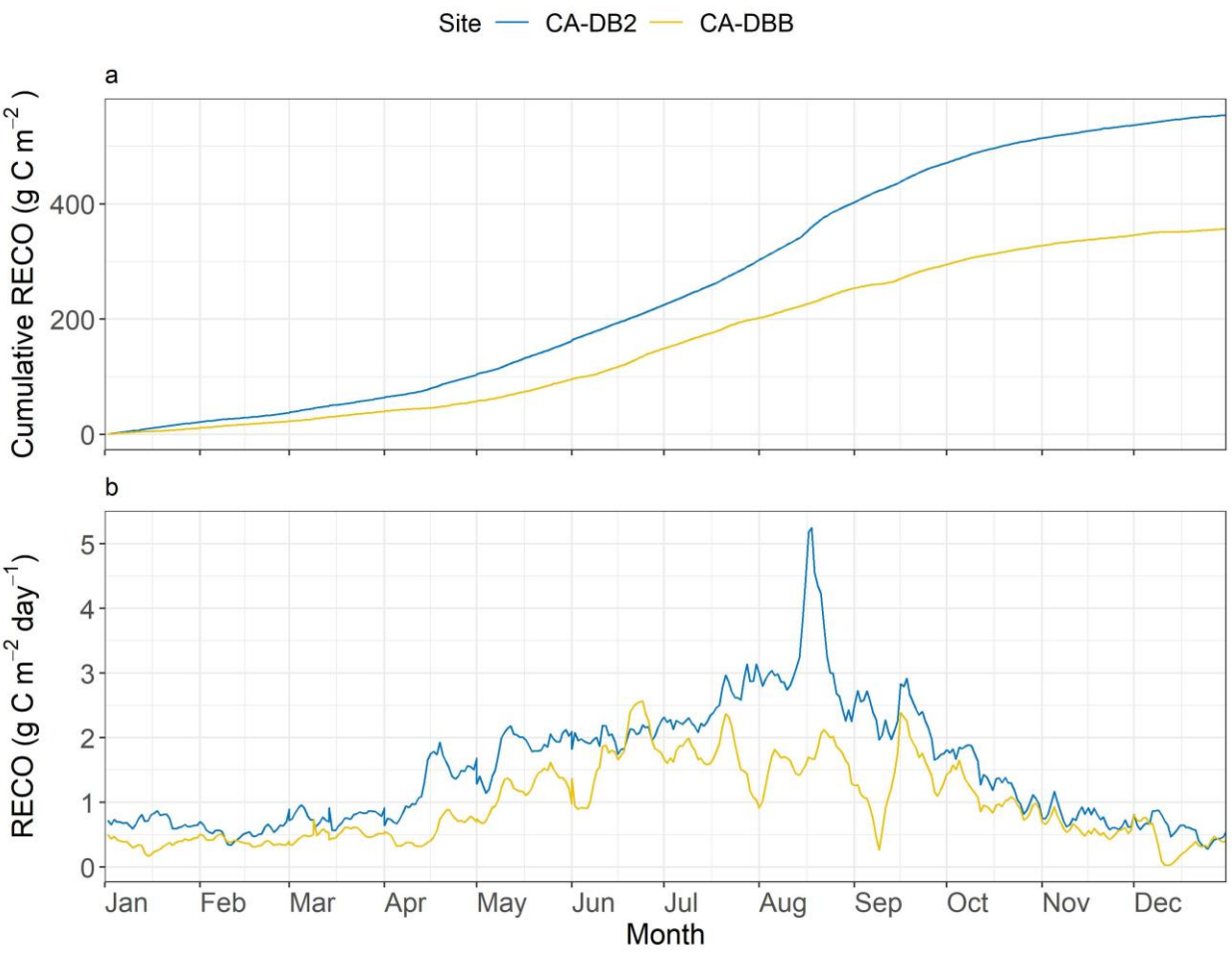

Figure 10. Cumulative night time modelled ecosystem respiration (RECO) (a) and daily RECO (b) over the duration of the study period in 2020 at CA-DB2 and CA-DBB.

3.3 FCH4

Annual CH_4 flux (FCH4) was higher at CA-DBB (12.8 ± 0.6 g C-CH_4 m^{-2}) than CA-DB2 (11.8 ± 1 g C-CH_4 m^{-2}) (Table 2; Fig. 11a). In the growing season, FCH4 was 28% higher at CA-DBB (10.5 ± 0.3 g C-CH_4 m^{-2}) than at CA-DB2 (8.2 ± 1.1 g C-CH_4 m^{-2}) (Table 2; Fig 11b.) and daily FCH4 increased throughout the growing season at both sites (Fig. 11b) with FCH4 peaking in August at both CA-DBB (2.8 g C-CH_4 $m^{-2}mon^{-1}$) and CA-DB2 (2.3 g C-CH_4 m^{-2}). During the growing season, daily mean fluxes were 57.3 mg C-CH_4 m^{-2} day^{-1} and 44.7 mg C-CH_4 m^{-2} day^{-1} at CA-DBB and CA-DB2, respectively. In the non-growing season, FCH4 at CA-DB2 (3.6 ± 0.5 g C-CH_4 m^{-2}) was significantly higher than at CA-DBB (2.4 ± 0.6 g C-CH_4 m^{-2}) (Table 2), and daily mean fluxes were 12.8 mg C-CH_4 m^{-2} day^{-1} and 19.6 mg C-CH_4 m^{-2} day^{-1} at CA-DBB and CA-DB2, respectively. Within sites, non-growing season total FCH4 at CA-DB2 was just less than half its growing season value; however, at CA-DBB it was less than a quarter of its growing season value (Table 2). Thus, there is a greater increase in FCH4 between the non-growing season and the growing season at CA-DBB than at CA-DB2.

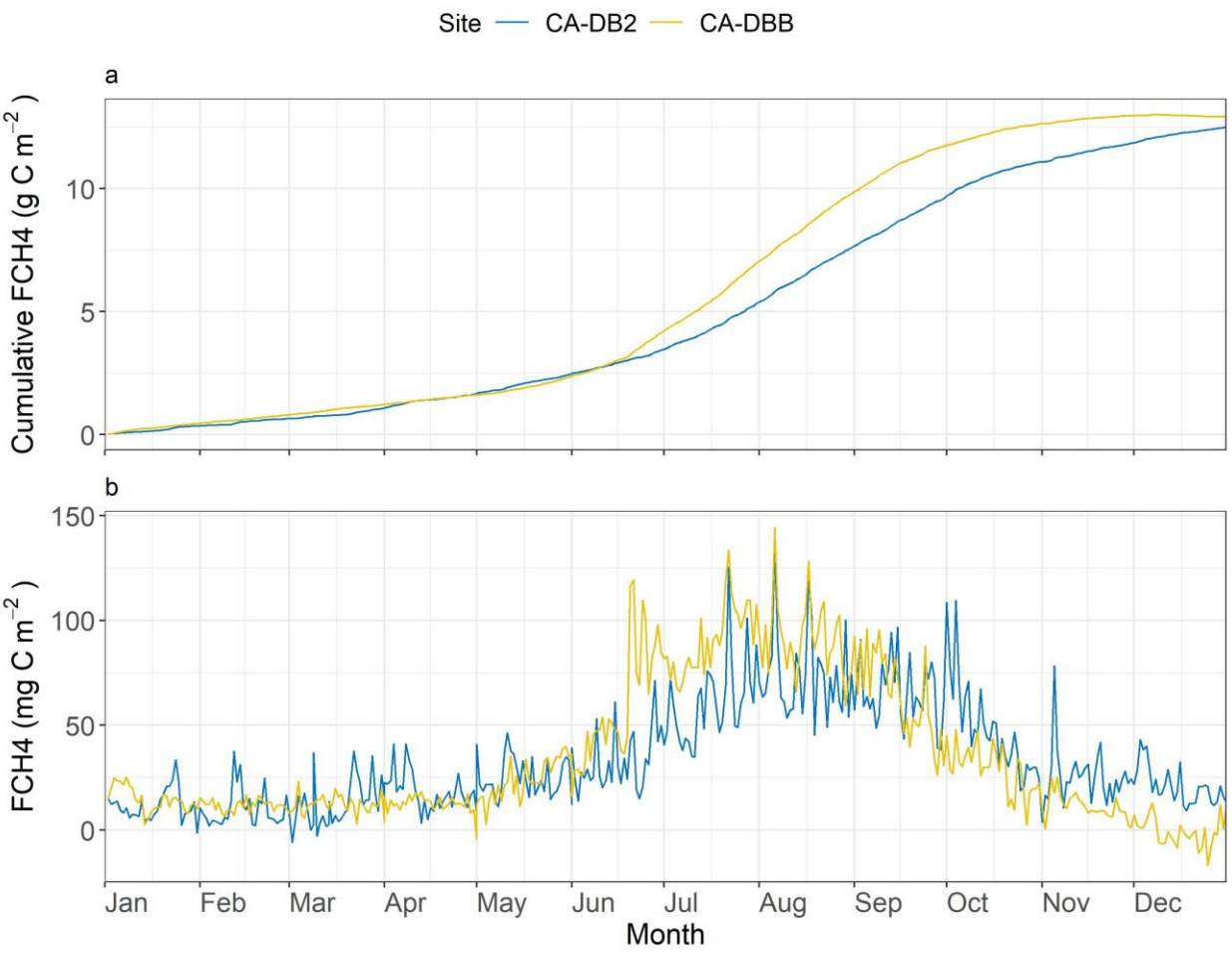

Figure 11. Cumulative methane flux (FCH4) (a) and daily mean FCH4 (b) over the duration of the study period in 2020at CA-DBB and CA-DB2.

Table 2 Annual, growing season, and non-growing season NEE, nighttime partitioned CO2 fluxes and FHC4 at CA-DBB and CA-DB2. * indicates statistically significant differences between sites. Values in brackets are the 95% confidence interval.

Site	Annual	Growing season	Non-growing season
NEE (g C-CO_2 m^{-2})			
CA-DBB	-26.2 (± 16.1)	-74 (± 5.8)	47.8 (± 6.9)
CA-DB2	27.4 (± 18.1) *	-32.8 (± 4.6) *	60.2 (± 7.3)
GPP (g C-CO_2 m^{-2})			
CA-DBB	387.8 (± 39.4)	329.6 (± 28.2)	58.1 (± 51.6)
CA-DB2	518.3 (± 11.1) *	438.8 (± 28.6) *	79.5 (± 16.5)
RECO (g C-CO_2 m^{-2})			
CA-DBB	361.5 (± 44.5)	255.7 (± 34)	105.9 (± 56.9)
CA-DB2	545.6 (± 11.4) *	406 (± 27.6) *	139.6 (± 10.9)
FCH4 (g C-CH_4 m^{-2})			
CA-DBB	12.8 (± 0.6)	10.5 (± 0.3)	2.4 (± 0.6)
CA-DB2	11.8 (± 1)	8.2 (± 1.1) *	3.6 (± 0.5) *

3.4 Radiative balance

Calculation of the GHG exchanges, when weighted by their sustained global warming potential (SGWP), indicates that both sites had a positive radiative balance on both 20 and 100- year time horizons. This is despite CA-DBB being a CO_2 sink by the end of the study period implying that the annual value of FCH4, when weighted by the SGWP, resulted in a positive radiative balance for the site. As CH_4 has a shorter atmospheric lifetime, yet higher SGWP, on a 20-year time horizon, the radiative balance of the sites is much higher than the 100-year time horizon (Table 3). On a 20-year time horizon, the radiative balance was 1501.3 ± 139.9 g CO_2-eq m^{-2} yr^{-1} and 1567 ± 193.2 g CO_2-eq m^{-2} yr^{-1} at CA-DBB and CA-DB2, respectively, compared to 627.8 ±

96.9 g CO_2-eq m^{-2} yr^{-1} and 764.9 ± 125.8 g CO_2-eq m^{-2} yr^{-1} at CA-DBB and CA-DB2, respectively, for the 100-year time horizon. In both scenarios CA-DB2 has a higher radiative balance, despite having lower annual FCH4. As CA-DB2 was a CO_2 source, this suggests that maintaining CO_2 sink status is vital in order to reduce the radiative balance, however, even with CO_2 sink status, FCH4 as observed at CA-DBB will result in a positive radiative balance.

Table 3. Radiative balance (g CO_2-eq m^{-2} yr^{-1}) and contribution of NEE (g CO_2-eq m^{-2} yr^{-1}) and FCH_4 (g CO_2-eq m^{-2} yr^{-1}) to the radiative balance on a 20-year and 100-year time horizon. A sustained global warming potential for FCH4 of 96 was used for the 20-year time horizon and 45 for the 100-year time horizon.

Site	20-year time horizon	100-year time horizon	NEE	CH_4
CA-DBB	1501.3 ± 139.9	627.8 ± 96.9	-143 ± 59	17.1 ± 0.84
CA-DB2	567 ± 193.2	764.9 ± 125.8	57.1 ± 66.3	15.7 ± 1.3

3.5 Environmental controls on CO_2 fluxes

3.5.1 RECO

At both sites, RECO increased with 5-cm soil temperature (TS) as expected, and the analysis of covariance (ANCOVA) showed that the relationship between daily RECO and TS differed significantly between sites (ANCOVA; $p < 0.05$). TS explained 65% and 91% of the variation in RECO at CA-DBB and CA-DB2, respectively (Table 4; Fig 12a). Furthermore, the apparent annual temperature sensitivity of RECO (Q10) was 10% higher at CA-DBB (3.3) than at CA-DB2 (3) (Table 4; Fig. 12a), implying a stronger temperature response at CA-DBB. When analysed as a single response variable, WTH had a negative relationship to RECO at both sites, whereby soil drying led to increased respiration. The effect of WTH on RECO differed

significantly between sites (ANCOVA; $p < 0.05$) and WTH explained more variation in RECO at CA-DB2 ($R^2 = 0.63$; $p < 0.05$) than at CA-DBB ($R^2 = 0.43$; $p < 0.05$) (Table 4; Fig. 12b). By comparing single linear models with one that included both variables, corrected Akaike Information Criterion (AICc) indicated the best fit model for RECO at CA-DBB only included TS, however, this was only slightly better than the model including both variables. At CA-DB2, however, the model with the best fit, according to AICc, was the model that included both TS and WTH (Table 4; Fig. 13a & b).

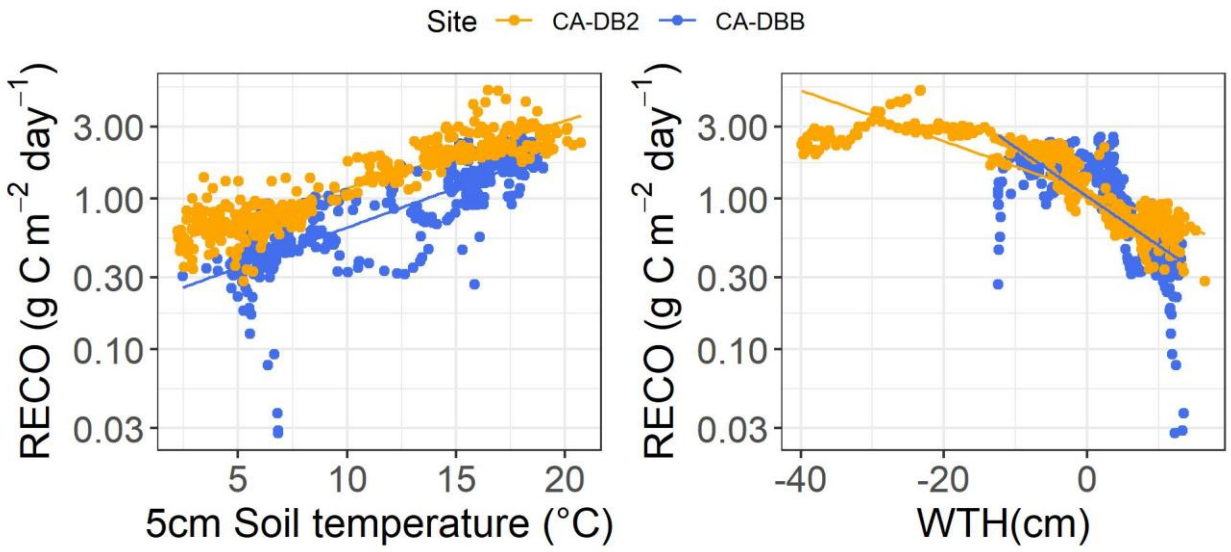

Figure 12. Daily mean night time modelled ecosystem respiration (RECO) response to 5-cm soil temperature (a) and water table height (b) at CA-DB2 and CA-DBB. Lines represent linear regression between variables.

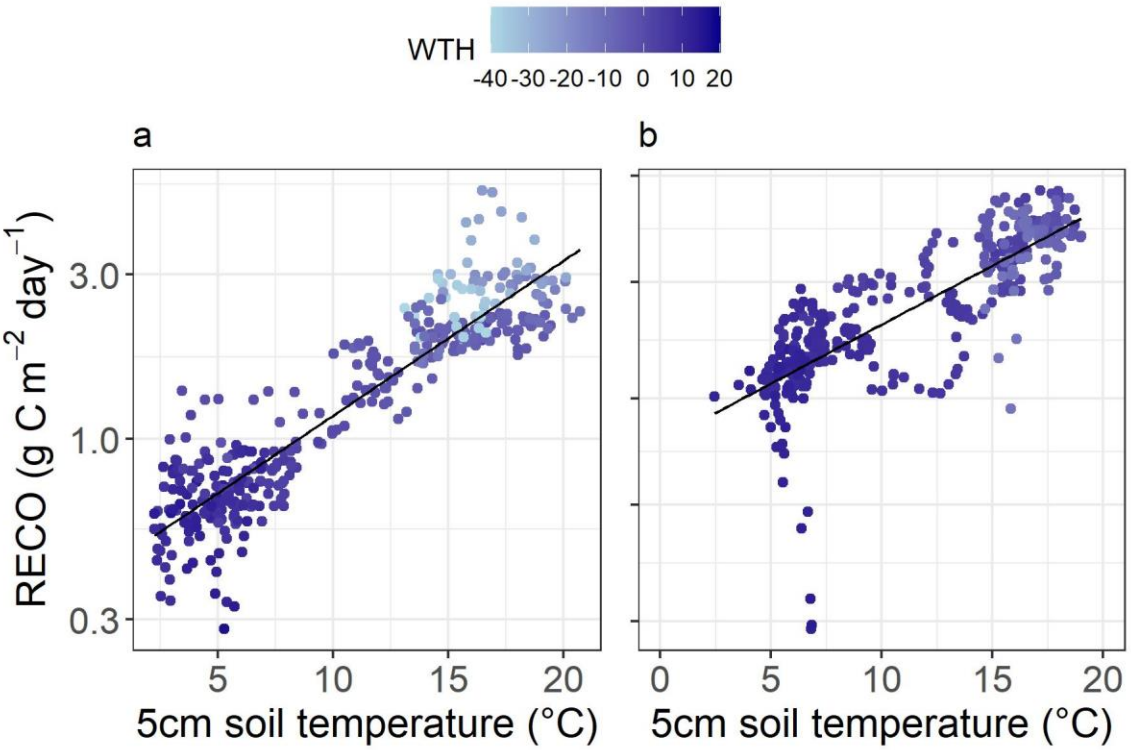

Figure 13. Daily ecosystem respiration (RECO) response to 5-cm soil temperature and water table height at (a) CA-DB2 and (b) CA-DBB.

Table 4. Regression model results and estimated Q10s for the response of logged ecosystem respiration to 5cm soil temperature (TS) and water table height (WTH). $^{n.s.}$ indicates non-significant predictor variables. Goodness of fit (R^2), rooted mean square error (RMSE) with degrees of freedom (df) and AICc (Akaike Information Criterion) are shown for each model.

Site	Model	R^2	RMSE (df)	AICc	Q10
CA-DBB					
lnRECO	= -1.64 + 0.1(TS)	0.65	0.43 (364)	430.8	3.3
lnRECO	= 0.04 $^{n.s.}$ – 0.07(WTH)	0.43	0.6 (364)	612.3	
lnRECO	= -1.58 + 0.12(TS) – 0.004(WTH)$^{n.s.}$	0.65	0.43 (363)	432.3	
CA-DB2					
lnRECO	= -1 + 0.11(TS)	0.91	0.2 (364)	-135.1	3
lnRECO	= 0.08 – 0.04(WTH)	0.63	0.4 (364)	373.9	
lnRECO	= -0.83 + 0.09(TS) – 0.01(WTH)	0.92	0.18 (363)	-221.6	

3.5.2 GPP

The GPP-PAR response was estimated for the growing season and non-growing season separately for each site. In the growing season, the initial slope for the light response curve (α) was 39% higher at CA-DB2 (0.025 μmol CO_2 (μmol photon)$^{-1}$) than CA-DBB (0.018 μmol CO_2 (μmol photon)$^{-1}$), which was expected considering the higher NDVI values throughout the year at CA-DB2 (Table 5; Fig. 14a). Conseqently, the maximum GPP (GPP_{max}), i.e. maximum CO_2 uptake when there were no light limitation at CA-DB2 was approximately 30% higher (6.25 μmol^{-1} m^{-2} s^{-1} at CA-DBB and 4.81 μmol^{-1} m^{-2} s^{-1} at CA-DB2) (Table 5; Fig. 14a). In the non-growing season, α was more similar between sites, 0.010 μmol CO2 (μmol photon)$^{-1}$and 0.011 CO_2 μmol CO2 (μmol photon)$^{-1}$ at CA-DBB and CA-DB2, respectively and non-growing season

GPP_{max} was 53% higher at CA-DB2 (2.81 μmol^{-1} m^{-2} s^{-1}) than at CA-DBB (1.84 μmol^{-1} m^{-2} s^{-1} a CA-DB2) (Table 5; Figure 14b).

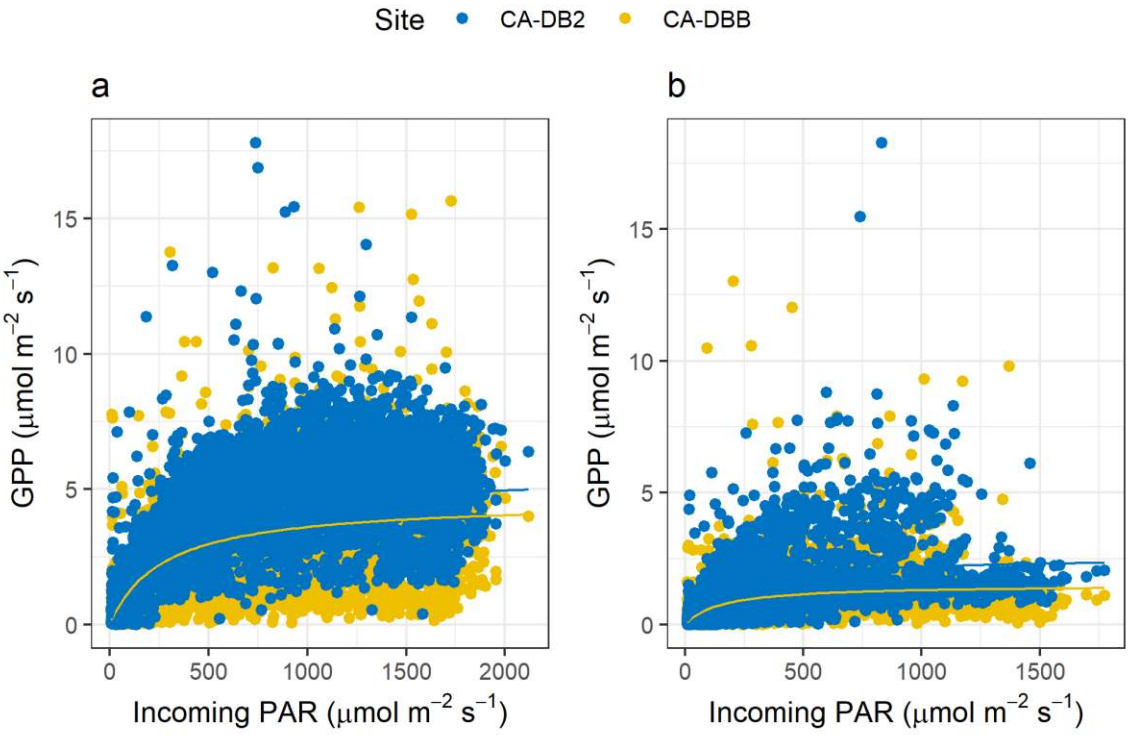

Figure 14. Rectangular hyperbolic light response curve for the growing season (a) and non-growing season (b) at CA-DBB and CA-DB2.

Table 5. Coefficients and model parameters for the rectangular hyperbolic light response curve at each site in the growing and non-growing season. α is the initial slope for the light response curve (μmol CO2 (μmol photon)$^{-1}$), GPP_{max} is the maximum GPP at light saturation (μmol^{-1} m^{-2} s^{-1}), RMSE (df) is the root mean square error with degrees of freedom.

Site	α	GPP_{max}	RMSE (df)	Period
CA-DBB	0.018	4.81	1.57 (5212)	GS
	0.010	1.84	0.89 (3191)	NGS
CA-DB2	0.025	6.25	1.42 (5344)	GS
	0.011	2.81	1.09 (3030)	NGS

3.6 Environmental controls on FCH4

When assessing the response of FCH4 to individual environmental variables, TS, WTH and GPP all explained more variation in FCH4 at CA-DBB than at CA-DB2 (Table 6). At both sites, TS was significantly correlated with and promoted FCH4, and at CA-DBB, of the three predictor variables, it explained the most variation in daily FCH4 ($R^2 = 0.48$, $p<0.05$). In contrast, at CA-DB2, the FCH4 response to TS was not as strong as at CA-DBB and it explained only 31% of the variation in FCH4. Consequently, the temperature sensitivity (Q10) of FCH4 to TS was higher at CA-DBB (Q10 = 1.59), compared to that CA-DB2 (Q10 = 1.21) (Table 7; Fig. 15a).

Simple linear regression revealed that both sites demonstrated a negative relationship between FCH4 and WTH, whereby an increase in WTH led to a decrease in FCH4. More variation was explained by this relationship at CA-DBB ($R^2= 0.47$, $p<0.05$), than at CA-DB2 ($R^2= 0.37$, $p<0.05$) (Table 6; Fig. 15b), and for CA-DB2, WTH explained more variation than other

individual variables. Using a non-linear response, however, reveals more about the relationship between FCH4 and WTH. At CA-DBB, FCH4 increased as WTH rose to just below the soil surface, where it peaked (F_{max}) at -6.68 cm (115.89 mg CH_4 m^{-2} day^{-1}) (Table 7). After this point, further increases in WTH led to a decrease in FCH4 (Fig. 15b.). In contrast, at CA-DB2, F_{max} was lower, at -29.32 cm (89.77 mg CH_4 m^{-2} day^{-1}) (Fig 15b; Table 7). Thus, at both sites, the estimated optimal WTH for F_{max} was below the soil surface; however, it was approximately 4 times higher, i.e., wetter at CA-DBB than at CA-DB2. The non-linear model also revealed that FCH4 occurred over a wider WTH range at CA-DB2 (24.01 cm) than CA-DBB (7.91 cm), as indicated by the water table amplitude (tR) (Table 7).

When considering the effect of GPP alone, both sites demonstrated a significant positive relationship with FCH4 (Table 6; Fig. 15c). However, the effect of GPP was slightly stronger at CA-DBB than at CA-DB2 and it explained more than twice the amount of variation at CA-DBB (R^2= 0.34, $p<0.05$) than at CA-DB2 (R^2= 0.16, $p<0.05$) (Table 6). This suggests that GPP plays a more important role in driving FCH4 at CA-DBB than at CA-DB2 (Table 6; Fig. 15c).

For both sites, multiple linear regression models were also tested, and the best two and 3 variable models were compared and ranked alongside the single linear models using AICc (Table 6). At both sites, the model that included all three variables (TS, WTH, and lnGPP), and a lnGPP x TS interaction term had the lowest AICc value and was therefore deemed the model that best explained FCH4. This model explained 61% of the variation at CA-DBB, but only 43% at CA-DB2. The next best model at both sites was one that included both TS and WTH. At CA-DBB

the model included a TS x WTH interaction, however, at CA-DB2, there was no interaction between TS and WTH (Table 6; Fig. 16a & b).

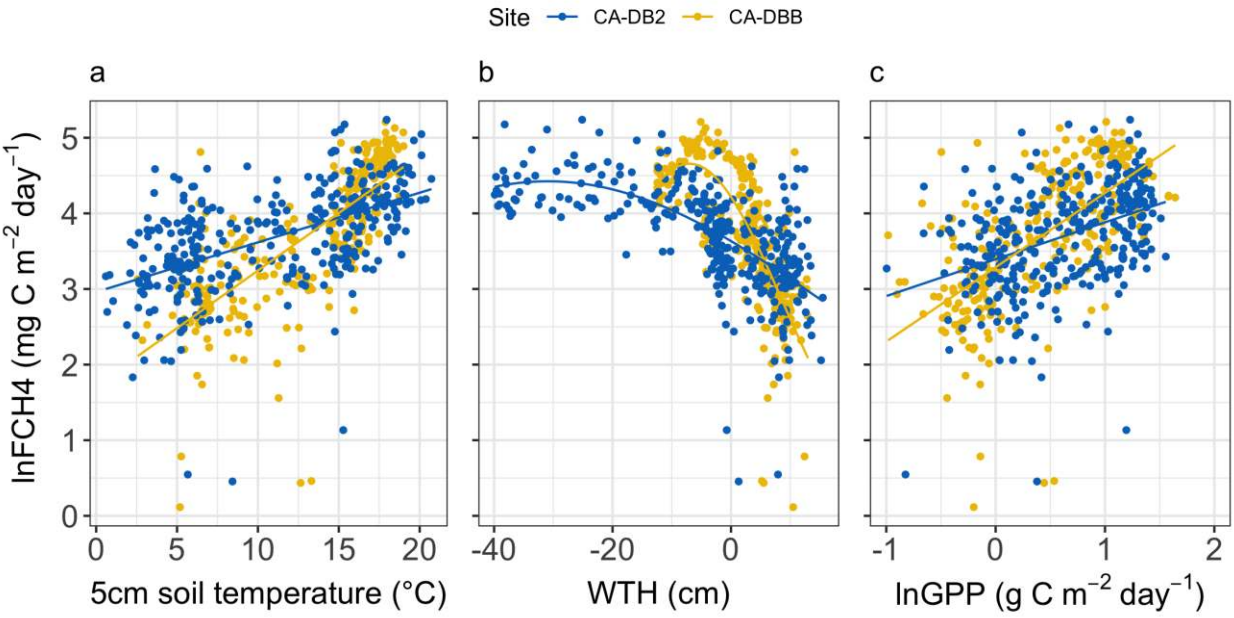

Figure 15. Daily methane flux (FCH4) response to daily mean (a) 5-cm soil temperature, (b) water table height (WTH), and daily GPP at CA-DB2 and CA-DBB.

Table 6. Results from regression analysis on daily mean FCH4 throughout the study period for the response of *F*CH4 (mg CH_4 m^{-2} day^{-1}) to 5-cm soil temperature (TS) (°C), water table height (WTH) (cm), and natural logarithm of GPP (lnGPP) (g CO_2 m^{-2} day^{-1}). $^{n.s.}$ indicates non-significant predictor variables. Goodness of fit (R^2), root mean square error (RMSE) with degrees of freedom (df) and AIC (Akaike Information Criterion) are shown for each model. +8 and +20 are offsets for lnFCH4.

Site	Model	R^2	RMSE (df)	AICc
CA-DBB				
ln ($FCH4_{+8}$)	= 3.23 +1(lnGPP)	0.34	0.8 (271)	657.9
ln ($FCH4_{+8}$)	= 3.90 - 0.1(WTH)	0.47	0.72 (272)	600.1
ln ($FCH4_{+8}$)	= 1.7 + 0.15(TS)	0.48	0.71 (272)	594.4
ln ($FCH4_{+8}$)	= 1.55 + 0.16(TS) + 0.08(WTH) – 0.009(TS*WTH)	0.57	0.64 (270)	543.1
ln ($FCH4_{+8}$)	=3.16 – 1.46(lnGPP) + 0.03(TS)$^{n.s.}$ – 0.07(WTH) + 0.12(lnGPP*TS)	0.61	0.61 (268)	517.8
CA-DB2				
ln ($FCH4_{+20}$)	= 3.36 + 0.48 (lnGPP)	0.16	0.65 (332)	661.8
ln ($FCH4_{+20}$)	= 2.9 + 0.07(TS)	0.31	0.59 (332)	598.5
ln ($FCH4_{+20}$)	= 3.56 – 0.03(WTH)	0.37	0.56 (332)	569.5
ln ($FCH4_{+20}$)	= 3.25 + 0.03(TS) – 0.02 (WTH)	0.39	0.55 (331)	555.6
ln ($FCH4_{+20}$)	= 3.15 – 0.52(lnGPP) – 0.06(TS) – 0.22(WTH) + 0.01(lnGPP*TS) $^{n.s.}$	0.43	0.54 (429)	542.5

Table 7. Estimated parameters for the non-linear FCH4 response to water table height and the estimated temperature sensitivity of FCH4 (Q10). Fmax is the estimated maximum FCH_4 at the optimal water table position (mg CH_4 m^{-2} day^{-1}), uR is the estimated optimal water table position for FCH_4 (cm), and tR is an estimate of the water table amplitude (cm) and root mean square error (RMSE) with df.

Site	Fmax (mg CH_4 m^{-2} day^{-1})	uR (cm)	tR (cm)	RMSE (df)	Q10	RMSE (df)
CA-DBB	115.89	-6.68	7.91	24.92 (271)	1.59	0.59 (272)
CA-DB2	89.77	-29.32	24.38	24.01 (331)	1.21	0.57 (332)

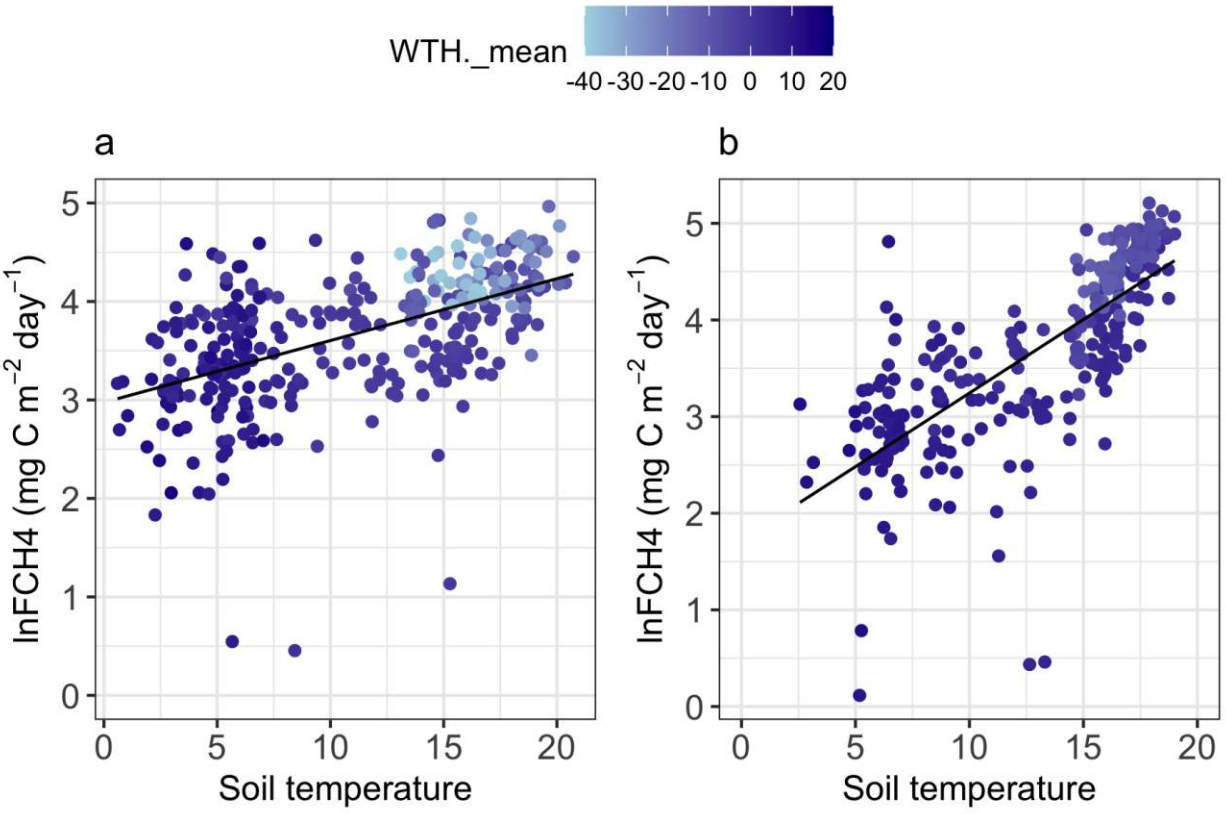

Figure 16. Daily mean log methane flux (lnFCH4) response to soil temperature and water table height at CA-DB2 (a) and CA-DBB (b).

Chapter 4: Discussion

The overarching aim of this study was to investigate how C and GHG dynamics vary in restored peatlands with different restoration strategies and environmental conditions, in particular, WTH. I evaluated the extent to which enhanced CO_2 uptake was offset by CH_4 emissions following restoration, and assessed environmental controls on NEE and its components, GPP and RECO, and FCH4 to help identify which environmental conditions maximise C uptake whilst minimizing GHG emissions. As WTH, TS and GPP are well-known to control C dynamics and GHG exchange in peatlands (Olefeldt et al., 2017; Turetsky et al., 2014), they were used together with CO_2 and CH_4 fluxes to investigate these questions. As restoration techniques varied between study sites, the two sites differed significantly in WTH, with CA-DBB undergoing active re-wetting and CA-DB2 with minimal, mostly passive rewetting, and hence both sites also differed in vegetation type. Consequently, CO_2 and CH_4 fluxes responded differently to other key environmental variables, notably TS, and GPP, within each site.

4.1 CO_2 budget and environmental effects on CO_2 fluxes

In 2020, cumulative NEE indicated that CA-DBB was a CO_2 sink (-26.2 ± 16.1 g C-CO_2 m^{-2}) by the end of the study period; however, CA-DB2 was a CO_2 source on an annual basis (27.4 ± 18.1 g C-CO_2 m^{-2}). At both Burns Bog sites, NEE is comparable to other temperate peatlands, both rewetted and natural (Evans et al., 2021; Lund et al., 2009; Strilesky and Humphreys, 2012). Both sites were growing season CO_2 sinks with values of -74 ± 5.8 g C-CO_2 m^{-2} at CA-DBB and -32.8 ± 4.6 g C-CO_2 m^{-2} , comparable to other rewetted peatlands (Waddington et al., 2010;

Tuittila et al., 1999). In the non-growing season, both sites were CO_2 sources to the atmosphere, (47.8 ± 6.9 g C-CO_2 m^{-2} and 60.2 ± 7.3 g C-CO_2 m^{-2} at CA-DBB and CA-DB2, respectively), as GPP decreased and was exceeded by RECO, an expected response during this period in peatlands (Nugent et al., 2018; Lafleur et al., 2001). However, it's important to note that substantial interannual variability in NEE is expected due to variations in RECO and GPP which will then affect CO_2 source or sink status of the ecosystem (Nugent et al., 2018; Lafleur et al., 2003).

Partitioning of NEE into RECO and GPP revealed that the driving process leading to the overall CO_2 budget differed between sites, following an expected trend considering the difference in WTH between sites. At CA-DBB, GPP dominated NEE, likely an effect of the high WTH throughout the year, supressing RECO (Pugh et al., 2018; Lund et al., 2009) and resulting in higher net CO_2 uptake. Thus, annual RECO at CA-DBB was approximately 49% lower than at CA-DB2. In contrast, at CA-DB2, RECO offset CO_2 uptake by GPP, leading to the site being a CO_2 source. Similar trends have been observed in both unrestored and some re-wetted peatlands as drier conditions promote RECO (Rankin et al., 2018; Wilson et al., 2016b), and therefore cancel out the effect of increased GPP. Whilst both sites had annual GPP values that fell into the range of other northern peatlands (Lund et al., 2009), GPP was significantly lower throughout the year at CA-DBB (387.3 ± 39.4.4 g C-CO_2 m^{-2}) than at CA-DB2 (518.3 ± 11.1 g C-CO_2 m^{-2}). As RECO was consistently higher at CA-DB2, this implies that RECO is offsetting the high GPP rates and therefore reducing the CO_2 sink potential. Considering the higher rates of GPP, NDVI, and thus vascular plant presence (Gavazov et al., 2018), coupled with drier soil conditions at CA-DB2, the higher rates of RECO are likely due to enhanced autotrophic, as well as

heterotrophic respiration due to the increase in labile substrate associated with plant productivity (Bengtson et al., 2012; Davidson and Janssens, 2006).

As I was interested in identifying the environmental conditions to minimize GHG emissions and maximize C uptake, two well-known drivers, soil temperature and WTH were used to assess ecosystem CO_2 dynamics (Loisel et al., 2020). When comparing single predictor variables using linear models, RECO had a strong positive relationship with TS at both sites, with TS explaining 65% and 91% of the variation in RECO at CA-DBB and CA-DB2, respectively. This temperature response is a well-established effect in peatland ecosystems (Lund et al., 2009). The temperature sensitivity (Q10) and TS coefficient in the linear model revealed that the soil temperature effect on RECO at CA-DBB was stronger than at CA-DB2, likely due to enhanced thermal conductivity of the wetter soil at CA-DBB (Mäkiranta et al., 2009).

As expected, RECO at both sites had a negative relationship with WTH, whereby a decrease in WTH led to an increase in RECO. This response to WTH was similar at each site; however, it explained 20% more variation in RECO at CA-DB2 than CA-DBB. Despite the significantly higher RECO at CA-DB2, the response to WTH at both sites supports findings in other studies that suggest re-wetting, even to different extents, as is the case at the two Burns Bog sites, is still likely to have a climate benefit in contrast to not re-wetting (Renou-Wilson et al., 2019; Holl et al., 2020). Moreover, sites that have not undergone re-wetting during post disturbance have been associated with high CO_2 emissions for at least a decade after extraction is stopped (Nugent et al., 2018).

As well as models with single predictor variables, multiple linear regression including both TS and WTH was used to assess RECO at the sites. At CA-DBB, the model with the best fit, as determined by AICc, was the TS model, however the AICc value was not much lower than the one including both TS and WTH. At CA-DB2, the model with the best fit for RECO included both variables. Whilst the coefficients were similar for both sites, WTH was not significant for CA-DBB, indicating that WTH plays a more important role in modulating the thermal conductivity and therefore also the temperature response of RECO at CA-DB2, an effect that was also observed by Mäkiranta et al., (2009). Further, both sites had Q10 values that were within the range of other temperate peatlands (Helfter et al., 2015; Silvola et al., 1996), and the relationship between lower WTH and decreasing Q10 values (Table 4), which was observed in this study, has been seen previously and explained by an increase in the ratio of heterotrophic to autotrophic respiration (Helfter et al., 2015; Dorrepaal et al., 2009). Hence, RECO is likely to be lower overall at CA-DBB because the WTH creates anaerobic conditions restricting both autotrophic and heterotrophic respiration.

GPP and NDVI were significantly higher annually and in the growing season at CA-DB2 than at CA-DBB. It's likely that the large decline in WTH (approximately 17 cm) at CA-DB2 in the growing season promoted plant growth (Pugh et al., 2018). A similar effect has been observed in a rewetted peatland whereby drought triggered fast colonization by pioneer species (Beyer et al., 2021). The GPP-PAR relationship demonstrates that both sites have GPP_{max} values within the range of other northern bog sites (Frolking et al., 1998), however, CA-DB2 has higher light use efficiency during the growing season, as indicated by the higher initial estimated slope (light use efficiency [LUE, α]) and GPP_{max}. For both sites, the increase in α and GPP_{max} follows the trend

in NDVI between the non-growing season and the growing season, and both have similar GPP_{max} values to other northern bog sites (Frolking et al., 1998). Despite the higher LUE and GPP_{max} at CA-DB2, it was still a CO_2 source by the end of the year and it's important to consider that in a warming climate it's possible that GPP could be stimulated further, leading to an enhanced CO_2 sink strength (Munir et al., 2015), or drive increased RECO (both heterotrophic and autotrophic) leading to less C being sequestered in the longer term and loss of soil C (Limpens et al., 2008).

4.2 FCH4 budget and environmental controls on FCH4 emissions

Annual FCH4 was higher at CA-DBB than CA-DB2 (12.8 ± 0.61 g C-CH_4 m^{-2} yr-1 and 11.8 ± 1 g C-CH_4 m^{-2} yr-1, respectively), and annual FCH4 values at both sites were within the range of natural and rewetted northern peatlands (Wilson et al., 2016b; Abdalla et al., 2016). Growing season FCH4 dominated the annual FCH4 budget at both sites due to warmer temperatures and higher GPP associated with the growing season (Chu et al., 2014). FCH4 was significantly higher at CA-DBB than at CA-DB2 in the growing season, but in the non-growing season, it was significantly higher at CA-DB2 (3.6 ± 0.5 g C-CH_4 m^{-2}) than at CA-DBB (2.4 ± 0.6 g C-CH_4 m^{-2}). This may be due to the increase in WTH height at CA-DB2, which was on average 17.6 cm higher in the non-growing season than the growing season, compared to an 8.5 cm increase at CA-DBB. Thus, the higher observed fluxes at CA-DB2 during this period may be due to the fact that drier ecosystems are typically more sensitive to shifts in WTH than wet ecosystems, and the greater increase in WTH at CA-DB2 promoted higher FCH4 relative to CA-DBB (Olefeldt et al., 2017).

The key role of WTH, TS and GPP in FCH4 in peatlands has been widely demonstrated (Olefeldt et al., 2017; Zhu et al., 2020; Knox et al., 2016). When comparing the effect of single predictor variables on FCH4, TS explained the most variance (48%) and had the lowest AICc value at CA-DBB, in line with previous studies that cite the strong control of temperature on FCH4 (Pugh et al., 2018; McNicol et al., 2020; Olefeldt et al., 2017; Christensen et al., 2003; Lai et al., 2014). However, at CA-DB2, TS explained just 31% of the variance, and was not the best single predictor model. Further, the temperature sensitivity of FCH4 was higher at CA-DBB (Q10 = 1.59) than at CA-DB2 (Q10 = 1.21), which again, is in agreement with other studies demonstrating that wetter ecosystems are more sensitive to changes in temperature than drier ecosystems (Olefeldt et al., 2017), and along with overall warmer TS, potentially explains why growing season FCH4 was so much higher at CA-DBB than at CA-DB2.

Whilst TS was the single environmental factor explaining most variance in FCH4 at CA-DBB, at CA-DB2, WTH explained the most variance (37%) and had the lowest AICc values out of the single predictor linear models. As mentioned previously, there is a difference between the dominant controls of FCH4 in wet vs. dry ecosystems. For instance, multiple studies have demonstrated that where the WTH is at or above the surface, temperature exerts the overarching control; however, where WTH is generally below the soil surface, WTH exerts more control (Olefeldt et al., 2017; Knox et al., 2019). Despite methanogenesis occurring in anaerobic conditions (Dean et al., 2018), at both sites, a drop in WTH was associated with an increase in emissions, an inverse relationship which has been observed previously in other northern peatlands (Bellisario et al., 1999; Brown et al., 2014; Beyer et al., 2021; Lai et al., 2014). This is likely due to the confounding effect of temperature, whereby the lower WTH in the growing

season correlated with higher temperatures, which promoted FCH4, or a decrease in hydrostatic pressure promoting ebullition leading to CH_4 release (Beaulieu et al., 2018; Strack et al., 2006). In contrast, when the WTH is higher, it is often associated with colder temperatures and therefore methanogenesis is restricted. Whilst these relationships largely represent the seasonal response of FCH4 to WTH, it is important to note on an annual timescale, the higher water table at CA-DBB led to overall higher annual FCH4.

To better explain the relationship between FCH4 and WTH, it was modelled using a non-linear function commonly used in the literature (Olefeldt et al., 2017; Turetsky et al., 2014). The non-linear model allowed identification of the optimal WTH for maximum FCH4, which was below the soil surface at both sites. At CA-DB2, maximum FCH4 ($FCH4_{max}$) was 89.77 mg C-CH_4 m^{-2} day^{-1} and occurred when the WTH was -29.23 cm, and at CA-DBB, $FCH4_{max}$was 115.89 mg C-CH_4 m^{-2} day^{-1} and it occurred when WTH was -6.68 cm, a WTH nearly four times higher than CA-DB2. The higher $FCH4_{max}$ at CA-DBB is likely because the site is wetter, which means the soil has a higher thermal admittance and therefore results in TS staying warmer for longer, thus promoting FCH4 to a higher degree (Turetsky et al., 2008). Despite the difference between sites, both report similar values to other northern peatlands, which implies there is substantial variation in the response of FCH4 to WTH (Abdalla et al., 2016; Turetsky et al., 2014). In addition to $FCH4_{max}$ and the WTH it occurs at, the non-linear model also reveals the WTH amplitude (tR), indicating whether FCH4 occurs within a narrow or broad range. At CA-DB2, FCH4 occurred over range that was twice as large as at CA-DBB. This is likely because at CA-DB2, there were large WTH drawdowns that were associated with warmer temperatures in the growing season, and additionally, the presence of hummocks and hollows at the site means the landscape is

interspersed with anaerobic microsites even when the WTH is low. Thus, it is important to consider that the relationship between WTH and FCH4 in peatlands that feature hummocks and hollows, as in the Burns bog sites, should be extrapolated carefully as there is likely to be substantial variation in WTH within a site due to microtopography (Bubier et al., 1993).

Whilst WTH and TS are clearly prominent drivers, the significant role of GPP in promoting FCH4 has also been established (Chu et al., 2014). This relationship has explained approximately half of the seasonal variation in FCH4 at a boreal peatland (Luan and Wu, 2014), and at CA-DBB and CA-DB2, GPP had a positive correlation with FCH4, explaining 34% and 16% of the variation in daily mean FCH4, respectively. This supports the role that photosynthesis and vascular plant presence has in driving FCH4, which has been observed previously (Pugh et al., 2018). This is potentially through the increased availability of substrate for methanogenesis (Lai et al., 2014) or through transport via aerenchymatous vegetation (Whiting and Chanton, 1992). Confirming the important role of GPP in driving FCH4, at both sites the best model as determined by AICc was one that included WTH and a GPP x TS interaction. These relationships, however, largely reflect the seasonal response of FCH4, whereby the decrease in WTH leading to increased FCH4 is confounded by the TS effect, and do not reflect the effect of WTH on annual FCH4, whereby CA-DBB, which had a higher WTH throughout the year, had higher overall FCH4.

Interestingly, annual and growing season FCH4 was higher at CA-DBB than at CA-DB2, but not in the non-growing season. During this period, FCH4 at CA-DB2 was significantly higher, despite WTH and TS being significantly higher at CA-DBB. To explain the higher FCH4 in the

non-growing season, there are multiple potential driving factors; 1.) FCH4 at CA-DB2 is more sensitive to shifts in WTH and the relative increase in WTH observed in the non-growing season, being larger than that at CA-DBB, led to increased FCH4 (Olefeldt et al., 2017); 2.) Increased vascular plant presence facilitated FCH4 transport (Le Mer and Roger, 2001); and 3.) It is possible there was a role for priming, whereby similarly to RECO, higher GPP in the growing season at CA-DB2 facilitated the availability of labile substrate available for methanogenesis, ultimately leading to a hysteresis effect (McNicol et al., 2020), with FCH4 peaking later in the growing season. To support the theory that growing season GPP promoted non-growing season FCH4, Mc Nicol et al., 2020 found an approximately linear increase in FCH4 with GPP and also identified that there was a hysteresis effect in that there were higher CH_4 emissions during the late growing season compared to the early growing season. Hysteresis in plant productivity and CH_4 emissions was also observed by Rinne et al., (2017) in a boreal oligotrophic fen. In the current study there is also some evidence of hysteresis, with FCH4 peaking later in the growing season than GPP, however as hysteresis wasn't extensively examined, these results suggest future work should investigate the response further.

4.3 Radiative balance

To assess the radiative balance of each site, annual CO_2 equivalents were calculated whereby FCH4 was weighted by its SGWP as specified by Neubauer and Megonigal (2015). In using this metric, we are assuming that there are sustained emissions of CO_2 eq. of GHGs, as opposed to a single pulse, represented by the GWP metric. For both sites, the GHG balance was positive, which is in line with other peatlands, both restored and natural (Taillardat et al., 2020; Petrescu et al., 2015). The GHG balance was calculated on both 20- and 100- year time horizons, which

captures the effect of CH_4 as an extremely potent GHG, especially on shorter time horizons. On 20- and 100- year time horizons the radiative balance of CA-DBB was 1501.3 ± 139.9 g CO_2-eq m^{-2} y^{-1} and 627.8 ± 96.9 g CO_2-eq m^{-2} y^{-1}, respectively, and 1567 ± 193.2 g CO_2-eq m^{-2} y^{-1} and 764.9 ± 125.8 g CO_2-eq m^{-2} y^{-1} at CA-DB2. Thus, despite having higher annual FCH4, the radiative balance of CA-DBB was less positive on both the 100- and 20-year time horizon than CA-DB2 and I can draw the conclusion, as others have, that long-term climate mitigation in peatlands needs to focus on reducing the CO_2 source strength since CH_4 is a short-lived gas (Tiemeyer et al., 2020). However, reducing FCH4 is still important, especially in the shorter term, considering its high SWGP. It should also be noted that calculation of the radiative balance does not include other GHG fluxes, e.g. N2O (although this was observed to be negligible across Burns Bog (A. Christen et al., 2016)), albedo or hydrologically exported fluxes. Additionally, these data are only representative of the 2020 trends in CO_2 and CH_4 dynamics and we would expect substantial variation inter-annually.

4.4 Management implications and re-wetted peatlands in a future climate

Based on results in the current study I've identified that CO_2 sink status is more important for the ecosystem than minimizing FCH4 in terms of long-term climate benefits, as the 100-year radiative balance was lower at CA-DBB, and thus has a smaller climate impact. This is due to the long atmospheric lifetime of CO_2, which could affect the climate centuries down the line. Thus, for future management when informing on how re-wetted peatlands can best be used as natural climate solutions, trends observed here suggest the focus should be on reducing RECO, i.e., prioritize WTH management for its effects on RECO as opposed to FCH4. However it will still be important to still minimize FCH4 where possible and optimize the WTH so as to avoid

the biogeochemical compromise associated with peatland rewetting (Hemes et al., 2018). Additionally, as CA-DBB had a lower radiative balance on a 100-year time horizon than CA-DB2, by emulating conditions of CA-DBB at CA-DB2, we could see a decrease in the radiative forcing and therefore a climate benefit.

It has already been suggested that moderate re-wetting that raises the water table to 10 – 20 cm below the soil surface would be the best way to prevent peat loss, without driving substantial CH_4 emissions (Ojanen and Minkkinen, 2020), and results from this study support this. In the growing season, when cumulative RECO is highest, at CA-DB2, the average WTH is -11.5 cm and it decreases to approximately -40 cm. In contrast, at CA-DBB the average growing season WTH is -0.4 cm, going down to -13 cm and RECO is lower. This suggests that the WTH at CA-DB2 should be raised and maintained to approximately the WTH of CA-DBB to decrease RECO, especially during the growing season. By maintaining this higher water table at CA-DB2, it is likely that RECO may even continue to decrease with further time (Holl et al., 2020), however a decrease in GPP has been observed in relation to increasing WTH in a northern hemisphere fen (Pugh et al., 2018) and thus may have cancelling effects on the impact of reduced RECO. However, when considering FCH4 as well, the non-linear response to WTH revealed that FCH4 peaks at approximately -7 cm at CA-DBB, thus suggesting that whilst the WTH should be raised at CA-DB2, at both sites it should not exceed approximately -7 cm, to avoid high FCH4. These suggestions for WTH management, however, are only based on the trends observed in 1 year of study, and therefore substantial variability is expected due to interannual variation in climate and CO_2 and FCH4.

When making management decisions and predicting future trends in C and GHG dynamics in these ecosystems, we must also consider what the future climate is predicted to be like. Zhu et al., 2020 established that mean CH_4 emissions increase as latitude decreases, implying that moving towards a warmer climate will drive enhanced CH_4 emissions from peatlands. Additionally, as the climate warms, we will likely experience longer growing seasons, and although GPP will likely increase, this will be partly offset by the increase in RECO (Lund et al., 2009) and could also promote FCH4. Besides temperature, future trends in precipitation also need to be considered, as this will have an important impact on modulating the WTH, especially in ombrotrophic bogs. In Metro Vancouver, the climate is predicted to get warmer, and by 2050 it is likely we will experience an average annual increase in daytime temperatures of 2.9 °C (Metro Vancouver, 2016). Additionally, we are predicted to experience wetter winters and drier summers (Metro Vancouver, 2016). This implies that without active water table management, we could see increased rates of RECO and FCH4 from these sites, ultimately leading to an increase in the radiative balance, which could drive a positive feedback in the land C- climate cycle and thus have a warming effect on the climate. Additionally, with warmer, drier summers, we are likely to see an increase in wildfire events, which would be detrimental to the ecosystem, destroying biodiversity and releasing large amounts of CO_2 into the atmosphere (Metro Vancouver, 2016; Page and Baird, 2016).

As well as the management implications directly derived from the results in this study, it can't go without saying that involvement with First Nations groups in the management of the Burns Bog sites, is lacking. With this in mind, multiple studies have demonstrated that nature conservancy is often more successful in land that is looked after and controlled by the Indigenous people of the

area (Frainer et al., 2020; Ogar et al., 2020). Thus, I think advocating for increased involvement with the First Nations groups at Burns Bog would be a logical next step in management of the site.

4.5 Study limitations and future work

The main limitation of this study is that it only represents one year of observations and significant interannual variability in C and GHG dynamics is expected. For example, studies have shown the shift towards a stronger CO_2 sink with time since restoration, suggesting the two Burns Bog sites may also head along this trajectory (Hambley et al., 2019). This variation is something to keep in mind when extrapolating results and making suggestions for future management. Another limitation is that WTH was only measured in one location, however both sites featured hummocks and hollows, implying that the microtopography within a site is likely to affect the WTH, and therefore extrapolation of results relating to WTH should be considered carefully. Additionally, whilst GPP, NDVI and a priori knowledge of plant community composition (Hebda et al., 2000) were used to communicate the greater vascular plant presence at CA-DB2, no surveys were done at the sites during the study period to confirm this.

Considering there is likely to be high inter-annual variability, future work should focus on investigating interannual variability in C and GHG dynamics within these sites, especially over longer time frames. This will give a better idea of future trends in the radiative balance and therefore better guidance for peatland restoration and management. Considering there was some evidence of hysteresis, further investigation into the hysteresis effect of GPP and FCH4 would also be beneficial to help predict future trends Finally, future work would also benefit from more

comprehensive vegetation surveys and more in-depth consideration of how plant community composition is affecting NEE and FCH4.

Chapter 5: Conclusions

By comparing the two Burns Bog sites that underwent different restoration processes and therefore had differing environmental conditions, in particular WTH, I was able to identify differences in C and GHG dynamics, as well their driving factors. RECO was predominately driven by TS at both sites, however there was also a significant role of WTH at CA-DB2, the drier site. The main control on FCH4 differed between each site, with TS explaining more variation in FCH4 at CA-DBB and WTH explaining more at CA-DB2, implying a difference between the main driver of FCH4 at wet vs. dry sites. At CA-DBB, which had a higher WTH throughout the study period than CA-DB2, annual FCH4 was greater, as expected. However, at CA-DBB, net CO_2 uptake was also higher and therefore led to the site being a CO_2 sink and having a lower GHG balance than CA-DB2. This was due to the consistently high WTH at CA-DBB, which restricted CO_2 loss (i.e., RECO) and permitted greater CO_2 uptake. In contrast, higher rates of RECO than GPP at CA-DB2 led to the site being a CO_2 source. This suggests that it is vital to maintain CO_2 sink status, and therefore we should focus rewetting efforts on those that reduce CO_2 loss, i.e., reduce WTH drawdown. However, it is also important to ensure that FCH4 emissions are minimized, to avoid the offsetting CO_2 uptake and resulting in a biogeochemical compromise, which could also have dire consequences for the climate.

In a future climate that is predicted to be warmer and drier, it is likely that re-wetting disturbed peatlands will have a climate benefit as opposed to not re-wetting due to reductions in RECO. Therefore, re-wetting is likely to represent a beneficial natural climate solution. However, these results suggest that restoring peatlands via re-wetting can still have variable results in terms of radiative balance and climate effects, and by comparing re-wetted peatlands with different

environmental conditions and at different restoration stages, we can identify those conditions that will lead to the most beneficial effect for the climate.

References

Abdalla, M., Hastings, A., Truu, J., Espenberg, M., Mander, U., and Smith, P.: Emissions of methane from northern peatlands: a review of management impacts and implications for future management options, 6, 7080–7102, https://doi.org/10.1002/ece3.2469, 2016.

Almagro, M., López, J., Querejeta, J. I., and Martínez-Mena, M.: Temperature dependence of soil CO2 efflux is strongly modulated by seasonal patterns of moisture availability in a Mediterranean ecosystem, 41, 594–605, https://doi.org/10.1016/j.soilbio.2008.12.021, 2009.

Alster, C. J., von Fischer, J. C., Allison, S. D., and Treseder, K. K.: Embracing a new paradigm for temperature sensitivity of soil microbes, Global Change Biology, 26, 3221–3229, https://doi.org/10.1111/gcb.15053, 2020.

Altor, A. E. and Mitsch, W. J.: Methane flux from created riparian marshes: Relationship to intermittent versus continuous inundation and emergent macrophytes, 28, 224–234, https://doi.org/10.1016/j.ecoleng.2006.06.006, 2006.

Altor, A. E. and Mitsch, W. J.: Methane and carbon dioxide dynamics in wetland mesocosms: Effects of hydrology and soils, 18, 1307–1320, https://doi.org/10.1890/07-0009.1, 2008.

Anderson, F. E., Bergamaschi, B., Sturtevant, C., Knox, S., Hastings, L., Windham-Myers, L., Detto, M., Hestir, E. L., Drexler, J., Miller, R. L., Matthes, J. H., Verfaillie, J., Baldocchi, D., Snyder, R. L., and Fujii, R.: Variation of energy and carbon fluxes from a restored temperate freshwater wetland and implications for carbon market verification protocols, 121, 777–795, https://doi.org/10.1002/2015jg003083, 2016.

Balcombe, P., Speirs, J. F., Brandon, N. P., and Hawkes, A. D.: Methane emissions: choosing the right climate metric and time horizon, Environ. Sci.: Processes Impacts, 20, 1323–1339, https://doi.org/10.1039/C8EM00414E, 2018.

Beaulieu, J. J., Balz, D. A., Birchfield, M. K., Harrison, J. A., Nietch, C. T., Platz, M. C., Squier, W. C., Waldo, S., Walker, J. T., White, K. M., and Young, J. L.: Effects of an Experimental Water-level Drawdown on Methane Emissions from a Eutrophic Reservoir, Ecosystems, 21, 657–674, https://doi.org/10.1007/s10021-017-0176-2, 2018.

Bellisario, L. M., Bubier, J. L., Moore, T. R., and Chanton, J. P.: Controls on CH4 emissions from a northern peatland, 13, 81–91, https://doi.org/10.1029/1998GB900021, 1999.

Bengtson, P., Barker, J., and Grayston, S. J.: Evidence of a strong coupling between root exudation, C and N availability, and stimulated SOM decomposition caused by rhizosphere priming effects, 2, 1843–1852, https://doi.org/10.1002/ece3.311, 2012.

Beyer, F., Jansen, F., Jurasinski, G., Koch, M., Schröder, B., and Koebsch, F.: Drought years in peatland rewetting: rapid vegetation succession can maintain the net CO_2 sink function, 18, 917–935, https://doi.org/10.5194/bg-18-917-2021, 2021.

Bhatti, J. S. and Tarnocai, C.: Influence of Climate and Land Use Change on Carbon in Agriculture, Forest, and Peatland Ecosystems across Canada, in: Soil Carbon Sequestration and the Greenhouse Effect, John Wiley & Sons, Ltd, 47–70, https://doi.org/10.2136/sssaspecpub57.2ed.c4, 2009.

Bridgham, S. D., Cadillo-Quiroz, H., Keller, J. K., and Zhuang, Q.: Methane emissions from wetlands: biogeochemical, microbial, and modeling perspectives from local to global scales, 19, 1325–46, https://doi.org/10.1111/gcb.12131, 2013.

Brown, M. G., Humphreys, E. R., Moore, T. R., Roulet, N. T., and Lafleur, P. M.: Evidence for a nonmonotonic relationship between ecosystem-scale peatland methane emissions and water table depth, Journal of Geophysical Research: Biogeosciences, 119, 826–835, https://doi.org/10.1002/2013JG002576, 2014.

Bubier, J. L., Moore, T. R., and Roulet, N. T.: Methane Emissions from Wetlands in the Midboreal Region of Northern Ontario, Canada, 74, 2240–2254, https://doi.org/10.2307/1939577, 1993.

Burba, G. and A.: A Brief Practical Guide to Eddy Covariance Flux measurements: Principles and Workflow Examples for Scientific and Industrial Applications, LI-COR Biosciences, Lincoln, Nebraska, 2010.

Butler, C.: From Reclamation to Conservation: A History of Settler Place-Making in Burns Bog, British Columbia, York University, Toronto, Ontario, Canada, 110 pp., 2019.

Carey, J. C., Tang, J., Templer, P. H., Kroeger, K. D., Crowther, T. W., Burton, A. J., Dukes, J. S., Emmett, B., Frey, S. D., Heskel, M. A., Jiang, L., Machmuller, M. B., Mohan, J., Panetta, A. M., Reich, P. B., Reinsch, S., Wang, X., Allison, S. D., Bamminger, C., Bridgham, S., Collins, S. L., de Dato, G., Eddy, W. C., Enquist, B. J., Estiarte, M., Harte, J., Henderson, A., Johnson, B. R., Larsen, K. S., Luo, Y., Marhan, S., Melillo, J. M., Penuelas, J., Pfeifer-Meister, L., Poll, C., Rastetter, E., Reinmann, A. B., Reynolds, L. L., Schmidt, I. K., Shaver, G. R., Strong, A. L., Suseela, V., and Tietema, A.: Temperature response of soil respiration largely unaltered with experimental warming, 113, 13797–13802, https://doi.org/10.1073/pnas.1605365113, 2016.

Chestnutt, C.: For peak's sake: A water balance study and comparison of the eddy covariance technique and semi-empirical calculation to determine summer evapotranspiration in Burn's Bog, British Columbia, The University of Edunburgh, The University of British Columbia, 2015.

Christen, A., Jassal, R. S., Black, T. A., Grant, Hawthorne, I., Johnson, M. S., Lee, S. C., and Merkens, M.: Summertime greenhouse gas fluxes from an urban bog undergoing restoration through rewetting, 1, https://doi.org/10.19189/MaP.2015.OMB.207, 2016.

Christensen, T. R., Ekberg, A., Ström, L., Mastepanov, M., Panikov, N., Öquist, M., Svensson, B. H., Nykänen, H., Martikainen, P. J., and Oskarsson, H.: Factors controlling large scale variations in methane emissions from wetlands, 30, https://doi.org/10.1029/2002GL016848, 2003.

Chu, H., Chen, J., Gottgens, J. F., Ouyang, Z., John, R., Czajkowski, K., and Becker, R.: Net ecosystem methane and carbon dioxide exchanges in a Lake Erie coastal marsh and a nearby cropland, Journal of Geophysical Research: Biogeosciences, 119, 722–740, https://doi.org/10.1002/2013JG002520, 2014.

Couwenberg, J., Thiele, A., Tanneberger, F., Augustin, J., Bärisch, S., Dubovik, D., Liashchynskaya, N., Michaelis, D., Minke, M., Skuratovich, A., and Joosten, H.: Assessing greenhouse gas emissions from peatlands using vegetation as a proxy, 674, 67–89, https://doi.org/10.1007/s10750-011-0729-x, 2011.

Davidson, E. A. and Janssens, I. A.: Temperature sensitivity of soil carbon decomposition and feedbacks to climate change, 440, 165–73, https://doi.org/10.1038/nature04514, 2006.

Dean, J. F., Middelburg, J. J., Röckmann, T., Aerts, R., Blauw, L. G., Egger, M., Jetten, M. S. M., de Jong, A. E. E., Meisel, O. H., Rasigraf, O., Slomp, C. P., in't Zandt, M. H., and Dolman, A. J.: Methane Feedbacks to the Global Climate System in a Warmer World, 56, 207–250, https://doi.org/10.1002/2017rg000559, 2018.

Burns Bog Overview: https://www.delta.ca/discover-delta/burns-bog/burns-bog-overview, last access: 13 May 2021.

Dieleman, C. M., Branfireun, B. A., and Lindo, Z.: Northern peatland carbon dynamics driven by plant growth form — the role of graminoids, 415, 25–35, https://doi.org/10.1007/s11104-016-3099-3, 2016.

Dorrepaal, E., Toet, S., van Logtestijn, R. S. P., Swart, E., van de Weg, M. J., Callaghan, T. V., and Aerts, R.: Carbon respiration from subsurface peat accelerated by climate warming in the subarctic, 460, 616–619, https://doi.org/10.1038/nature08216, 2009.

Evans, C. D., Peacock, M., Baird, A. J., Artz, R. R. E., Burden, A., Callaghan, N., Chapman, P. J., Cooper, H. M., Coyle, M., Craig, E., Cumming, A., Dixon, S., Gauci, V., Grayson, R. P., Helfter, C., Heppell, C. M., Holden, J., Jones, D. L., Kaduk, J., Levy, P., Matthews, R., McNamara, N. P., Misselbrook, T., Oakley, S., Page, S., Rayment, M., Ridley, L. M., Stanley, K. M., Williamson, J. L., Worrall, F., and Morrison, R.: Overriding water table control on managed peatland greenhouse gas emissions, 1–7, https://doi.org/10.1038/s41586-021-03523-1, 2021.

Frainer, A., Mustonen, T., Hugu, S., Andreeva, T., Arttijeff, E.-M., Arttijeff, I.-S., Brizoela, F., Coelho-de-Souza, G., Printes, R. B., Prokhorova, E., Sambou, S., Scherer, A., Shadrin, V., and Pecl, G.: Opinion: Cultural and linguistic diversities are underappreciated pillars of biodiversity, Proc Natl Acad Sci USA, 117, 26539, https://doi.org/10.1073/pnas.2019469117, 2020.

Frolking, S., Roulet, N., and Fuglestvedt, J.: How northern peatlands influence the Earth's radiative budget: Sustained methane emission versus sustained carbon sequestration, Journal of Geophysical Research: Biogeosciences, 111, https://doi.org/10.1029/2005JG000091, 2006.

Frolking, S. E., Bubier, J. L., Moore, T. R., Ball, T., Bellisario, L. M., Bhardwaj, A., Carroll, P., Crill, P. M., Lafleur, P. M., McCaughey, J. H., Roulet, N. T., Suyker, A. E., Verma, S. B., Waddington, J. M., and Whiting, G. J.: Relationship between ecosystem productivity and photosynthetically active radiation for northern peatlands, Global Biogeochemical Cycles 12, 115–126, https://doi.org/10.1029/97GB03367, 1998.

Gavazov, K., Albrecht, R., Buttler, A., Dorrepaal, E., Garnett, M. H., Gogo, S., Hagedorn, F., Mills, R. T. E., Robroek, B. J. M., and Bragazza, L.: Vascular plant-mediated controls on atmospheric

carbon assimilation and peat carbon decomposition under climate change, 24, 3911–3921, https://doi.org/10.1111/gcb.14140, 2018.

Griscom, B. W., Adams, J., Ellis, P. W., Houghton, R. A., Lomax, G., Miteva, D. A., Schlesinger, W. H., Shoch, D., Siikamäki, J. V., Smith, P., Woodbury, P., Zganjar, C., Blackman, A., Campari, J., Conant, R. T., Delgado, C., Elias, P., Gopalakrishna, T., Hamsik, M. R., Herrero, M., Kiesecker, J., Landis, E., Laestadius, L., Leavitt, S. M., Minnemeyer, S., Polasky, S., Potapov, P., Putz, F. E., Sanderman, J., Silvius, M., Wollenberg, E., and Fargione, J.: Natural climate solutions, Proc Natl Acad Sci USA, 114, 11645, https://doi.org/10.1073/pnas.1710465114, 2017.

Hambley, G., Andersen, R., Levy, P., Saunders, M., Cowie, N. R., Teh, Y. A., and Hill, T. C.: Net ecosystem exchange from two formerly afforested peatlands undergoing restoration in the Flow Country of northern Scotland, 23, 1–14, https://doi.org/10.19189/MaP.2018.DW.346, 2019.

Heathwaite, A. L.: Mires: process, exploitation and conservation., John Wiley & Sons Ltd, Chichester, x + 506 pp. pp., 1993.

Hebda, R. J., Gustavson, K., and Calder, A. M.: Burns Bog Ecosystem Review Synthesis Report for Burns Bog, Fraser River Delta, South-western British Columbia, Canada, Environmental Assessment Office, Victoria, BC, 2000.

Helfter, C., Campbell, C., Dinsmore, K. J., Drewer, J., Coyle, M., Anderson, M., Skiba, U., Nemitz, E., Billett, M. F., and Sutton, M. A.: Drivers of long-term variability in CO2 net ecosystem exchange in a temperate peatland, 12, 1799–1811, https://doi.org/10.5194/bg-12-1799-2015, 2015.

Hemes, K. S., Chamberlain, S. D., Eichelmann, E., Knox, S. H., and Baldocchi, D. D.: A Biogeochemical Compromise: The high methane cost of sequestering carbon in restored wetlands, 45, 6081–6091, https://doi.org/10.1029/2018gl077747, 2018.

Holl, D., Pfeiffer, E.-M., and Kutzbach, L.: Comparison of eddy covariance CO2 and CH4 fluxes from mined and recently rewetted sections in a northwestern German cutover bog, Biogeosciences, 17, 2853–2874, https://doi.org/10.5194/bg-17-2853-2020, 2020.

Hopple, A. M., Wilson, R. M., Kolton, M., Zalman, C. A., Chanton, J. P., Kostka, J., Hanson, P. J., Keller, J. K., and Bridgham, S. D.: Massive peatland carbon banks vulnerable to rising temperatures, Nature Communications, 11, 2373, https://doi.org/10.1038/s41467-020-16311-8, 2020.

Howie, S. A., Whitfield, P. H., Hebda, R. J., Munson, T. G., Dakin, R. A., and Jeglum, J. K.: Water Table and Vegetation Response to Ditch Blocking: Restoration of a Raised Bog in Southwestern British Columbia, 34, 381–392, https://doi.org/10.4296/cwrj3404381, 2009.

Joosten, H.: Wise use of mires: Background and principles, 239–250, 2003.

Kim, Y., Johnson, M. S., Knox, S. H., Black, T. A., Dalmagro, H. J., Kang, M., Kim, J., and Baldocchi, D.: Gap-filling approaches for eddy covariance methane fluxes: A comparison of three machine learning algorithms and a traditional method with principal component analysis, 26, 1499–1518, https://doi.org/10.1111/gcb.14845, 2020.

Knox, S. H., Sturtevant, C., Matthes, J. H., Koteen, L., Verfaillie, J., and Baldocchi, D.: Agricultural peatland restoration: effects of land-use change on greenhouse gas (CO2 and CH4) fluxes in the Sacramento-San Joaquin Delta, 21, 750–65, https://doi.org/10.1111/gcb.12745, 2015.

Knox, S. H., Matthes, J. H., Sturtevant, C., Oikawa, P. Y., Verfaillie, J., and Baldocchi, D.: Biophysical controls on interannual variability in ecosystem-scale CO2and CH4exchange in a California rice paddy, 121, 978–1001, https://doi.org/10.1002/2015jg003247, 2016.

Knox, S. H., Jackson, R. B., Poulter, B., McNicol, G., Fluet-Chouinard, E., Zhang, Z., Hugelius, G., Bousquet, P., Canadell, J. G., Saunois, M., Papale, D., Chu, H., Keenan, T. F., Baldocchi, D., Torn, M. S., Mammarella, I., Trotta, C., Aurela, M., Bohrer, G., Campbell, D. I., Cescatti, A., Chamberlain, S., Chen, J., Chen, W., Dengel, S., Desai, A. R., Euskirchen, E., Friborg, T., Gasbarra, D., Goded, I., Goeckede, M., Heimann, M., Helbig, M., Hirano, T., Hollinger, D. Y., Iwata, H., Kang, M., Klatt, J., Krauss, K. W., Kutzbach, L., Lohila, A., Mitra, B., Morin, T. H., Nilsson, M. B., Niu, S., Noormets, A., Oechel, W. C., Peichl, M., Peltola, O., Reba, M. L., Richardson, A. D., Runkle, B. R. K., Ryu, Y., Sachs, T., Schäfer, K. V. R., Schmid, H. P., Shurpali, N., Sonnentag, O., Tang, A. C. I., Ueyama, M., Vargas, R., Vesala, T., Ward, E. J., Windham-Myers, L., Wohlfahrt, G., and Zona, D.: FLUXNET-CH4 Synthesis Activity: Objectives, Observations, and Future Directions, Bulletin of the American Meteorological Society, 100, 2607–2632, https://doi.org/10.1175/BAMS-D-18-0268.1, 2019.

Laanbroek, H. J.: Methane emission from natural wetlands: interplay between emergent macrophytes and soil microbial processes. A mini-review, 105, 141–53, https://doi.org/10.1093/aob/mcp201, 2010.

Lafleur, P. M., Roulet, N. T., and Admiral, S. W.: Annual cycle of CO2 exchange at a bog peatland, Journal of Geophysical Research: Atmospheres, 106, 3071–3081, https://doi.org/10.1029/2000JD900588, 2001.

Lafleur, P. M., Roulet, N. T., Bubier, J. L., Frolking, S., and Moore, T. R.: Interannual variability in the peatland-atmosphere carbon dioxide exchange at an ombrotrophic bog, 17, https://doi.org/10.1029/2002GB001983, 2003.

Lai, D. Y. F., Moore, T. R., and Roulet, N. T.: Spatial and temporal variations of methane flux measured by autochambers in a temperate ombrotrophic peatland, 119, 864–880, https://doi.org/10.1002/2013JG002410, 2014.

Lazcano, C., Deol, A. S., Brummell, M. E., and Strack, M.: Interactive effects of vegetation and water table depth on belowground C and N mobilization and greenhouse gas emissions in a restored peatland, https://doi.org/10.1007/s11104-020-04434-2, 2020.

Le Mer, J. and Roger, P.: Production, oxidation, emission and consumption of methane by soils: A review, 37, 25–50, https://doi.org/10.1016/S1164-5563(01)01067-6, 2001.

Leroy, F., Gogo, S., Guimbaud, C., Bernard-Jannin, L., Hu, Z., and Laggoun-Défarge, F.: Vegetation composition controls temperature sensitivity of CO2 and CH4 emissions and DOC concentration in peatlands, 107, 164–167, https://doi.org/10.1016/j.soilbio.2017.01.005, 2017.

Limpens, J., Berendse, F., Blodau, C., Canadell, J. G., Freeman, C., Holden, J., Roulet, N., Rydin, H., and Schaepman-Strub, G.: Peatlands and the carbon cycle: from local processes to global implications – a synthesis, 5, 1475–1491, https://doi.org/10.5194/bg-5-1475-2008, 2008.

Loisel, J., Gallego-Sala, A. V., Amesbury, M. J., Magnan, G., Anshari, G., Beilman, D. W., Benavides, J. C., Blewett, J., Camill, P., Charman, D. J., Chawchai, S., Hedgpeth, A., Kleinen, T., Korhola, A., Large, D., Mansilla, C. A., Müller, J., van Bellen, S., West, J. B., Yu, Z., Bubier, J. L., Garneau, M., Moore, T., Sannel, A. B. K., Page, S., Väliranta, M., Bechtold, M., Brovkin, V., Cole, L. E. S., Chanton, J. P., Christensen, T. R., Davies, M. A., De Vleeschouwer, F., Finkelstein, S. A., Frolking, S., Gałka, M., Gandois, L., Girkin, N., Harris, L. I., Heinemeyer, A.,

Hoyt, A. M., Jones, M. C., Joos, F., Juutinen, S., Kaiser, K., Lacourse, T., Lamentowicz, M., Larmola, T., Leifeld, J., Lohila, A., Milner, A. M., Minkkinen, K., Moss, P., Naafs, B. D. A., Nichols, J., O'Donnell, J., Payne, R., Philben, M., Piilo, S., Quillet, A., Ratnayake, A. S., Roland, T. P., Sjögersten, S., Sonnentag, O., Swindles, G. T., Swinnen, W., Talbot, J., Treat, C., Valach, A. C., and Wu, J.: Expert assessment of future vulnerability of the global peatland carbon sink, Nature Climate Change, https://doi.org/10.1038/s41558-020-00944-0, 2020.

Luan, J. and Wu, J.: Gross photosynthesis explains the `artificial bias' of methane fluxes by static chamber (opaque versus transparent) at the hummocks in a boreal peatland, Environ. Res. Lett., 9, 105005, https://doi.org/10.1088/1748-9326/9/10/105005, 2014.

Lund, M., Lafleur, P. M., Roulet, N. T., Lindroth, A., Christensen, T. R., Aurela, M., Chojnicki, B. H., Flanagan, L. B., Humphreys, E. R., Laurila, T., Oechel, W. C., Olejnik, J., Rinne, J., Schubert, P., and Nilsson, M. B.: Variability in exchange of CO2 across 12 northern peatland and tundra sites, 16, no-no, https://doi.org/10.1111/j.1365-2486.2009.02104.x, 2009.

Mäkiranta, P., Laiho, R., Fritze, H., Hytönen, J., Laine, J., and Minkkinen, K.: Indirect regulation of heterotrophic peat soil respiration by water level via microbial community structure and temperature sensitivity, Soil Biology and Biochemistry, 41, 695–703, https://doi.org/10.1016/j.soilbio.2009.01.004, 2009.

McNicol, G., Knox, S. H., Guilderson, T. P., Baldocchi, D. D., and Silver, W. L.: Where old meets new: An ecosystem study of methanogenesis in a reflooded agricultural peatland, Global Change Biology, 26, 772–785, https://doi.org/10.1111/gcb.14916, 2020.

Metro Vancouver: Climate Projections for Metro Vancouver, 2016.

van der Molen, P. C. and Wijmstra, T. A.: The Thermal Regime of Hummock-Hollow Complexes on Clara Bog, Co. Offaly, 94B, 209–221, 1994.

Moore, T. R., Bubier, J. L., Frolking, S. E., Lafleur, P. M., and Roulet, N. T.: Plant biomass and production and CO2 exchange in an ombrotrophic bog, 90, 25–36, https://doi.org/10.1046/j.0022-0477.2001.00633.x, 2002.

Moreno-Mateos, D., Power, M. E., Comin, F. A., and Yockteng, R.: Structural and functional loss in restored wetland ecosystems, 10, e1001247, https://doi.org/10.1371/journal.pbio.1001247, 2012.

Munir, T. M., Perkins, M., Kaing, E., and Strack, M.: Carbon dioxide flux and net primary production of a boreal treed bog: Responses to warming and water-table-lowering simulations of climate change, 12, 1091–1111, https://doi.org/10.5194/bg-12-1091-2015, 2015.

Myhre, G.: Anthropogenic and Natural Radiative Forc- ing. In: Climate Change 2013: The Physical Science Basis. Contribution of Working Group I to the Fifth Assessment Report of the Intergovernmental Panel on Climate Change, Cambridge University Press, Cambridge, United Kingdom and New York, NY, USA., 2013.

Neubauer, S. C.: Global Warming Potential Is Not an Ecosystem Property, Ecosystems, https://doi.org/10.1007/s10021-021-00631-x, 2021.

Neubauer, S. C. and Megonigal, J. P.: Moving Beyond Global Warming Potentials to Quantify the Climatic Role of Ecosystems, 18, 1000–1013, https://doi.org/10.1007/s10021-015-9879-4, 2015.

Nugent, K. A., Strachan, I. B., Strack, M., Roulet, N. T., and Rochefort, L.: Multi-year net ecosystem carbon balance of a restored peatland reveals a return to carbon sink, 24, 5751–5768, https://doi.org/10.1111/gcb.14449, 2018.

Ogar, E., Pecl, G., and Mustonen, T.: Science Must Embrace Traditional and Indigenous Knowledge to Solve Our Biodiversity Crisis, 3, 162–165, https://doi.org/10.1016/j.oneear.2020.07.006, 2020.

Ojanen, P. and Minkkinen, K.: Rewetting Offers Rapid Climate Benefits for Tropical and Agricultural Peatlands But Not for Forestry-Drained Peatlands, Global Biogeochemical Cycles, 34, e2019GB006503, https://doi.org/10.1029/2019GB006503, 2020.

Olefeldt, D., Turetsky, M. R., Crill, P. M., and McGuire, A. D.: Environmental and physical controls on northern terrestrial methane emissions across permafrost zones, Global Change Biology, 19, 589–603, https://doi.org/10.1111/gcb.12071, 2013.

Olefeldt, D., Euskirchen, E. S., Harden, J., Kane, E., McGuire, A. D., Waldrop, M. P., and Turetsky, M. R.: A decade of boreal rich fen greenhouse gas fluxes in response to natural and experimental water table variability, 23, 2428–2440, https://doi.org/10.1111/gcb.13612, 2017.

Page, S. E. and Baird, A. J.: Peatlands and Global Change: Response and Resilience, Annu. Rev. Environ. Resour., 41, 35–57, https://doi.org/10.1146/annurev-environ-110615-085520, 2016.

Papale, D., Reichstein, M., Aubinet, M., Canfora, E., Bernhofer, C., Kutsch, W., Longdoz, B., Rambal, S., Valentini, R., Vesala, T., and Yakir, D.: Towards a standardized processing of Net Ecosystem Exchange measured with eddy covariance technique: algorithms and uncertainty estimation, 3, 571–583, https://doi.org/10.5194/bg-3-571-2006, 2006.

Petrescu, A. M., Lohila, A., Tuovinen, J. P., Baldocchi, D. D., Desai, A. R., Roulet, N. T., Vesala, T., Dolman, A. J., Oechel, W. C., Marcolla, B., Friborg, T., Rinne, J., Matthes, J. H., Merbold, L., Meijide, A., Kiely, G., Sottocornola, M., Sachs, T., Zona, D., Varlagin, A., Lai, D. Y., Veenendaal, E., Parmentier, F. J., Skiba, U., Lund, M., Hensen, A., van Huissteden, J., Flanagan, L. B., Shurpali, N. J., Grunwald, T., Humphreys, E. R., Jackowicz-Korczynski, M., Aurela, M. A., Laurila, T., Gruning, C., Corradi, C. A., Schrier-Uijl, A. P., Christensen, T. R., Tamstorf, M. P., Mastepanov, M., Martikainen, P. J., Verma, S. B., Bernhofer, C., and Cescatti, A.: The

uncertain climate footprint of wetlands under human pressure, 112, 4594–9, https://doi.org/10.1073/pnas.1416267112, 2015.

Pugh, C. A., Reed, D. E., Desai, A. R., and Sulman, B. N.: Wetland flux controls: how does interacting water table levels and temperature influence carbon dioxide and methane fluxes in northern Wisconsin?, 137, 15–25, http://dx.doi.org/10.1007/s10533-017-0414-x, 2018.

Rankin, T., Strachan, I. B., and Strack, M.: Carbon dioxide and methane exchange at a post-extraction, unrestored peatland, Ecological Engineering, 122, 241–251, https://doi.org/10.1016/j.ecoleng.2018.06.021, 2018.

Renou-Wilson, F., Moser, G., Fallon, D., Farrell, C. A., Müller, C., and Wilson, D.: Rewetting degraded peatlands for climate and biodiversity benefits: Results from two raised bogs, 127, 547–560, https://doi.org/10.1016/j.ecoleng.2018.02.014, 2019.

Rinne, J., Riutta, T., Pihlatie, M., Aurela, M., Haapanala, S., Tuovinen, J.-P., Tuittila, E.-S., and Vesala, T.: Annual cycle of methane emission from a boreal fen measured by the eddy covariance technique, 59, 449–457, https://doi.org/10.1111/j.1600-0889.2007.00261.x, 2017.

Roulet, N. T.: Peatlands, carbon storage, greenhouse gases, and the Kyoto Protocol: Prospects and significance for Canada., 20, 605–615, https://doi.org/doi: 10.1672/0277-5212(2000)020[0605:pcsgga]2.0.co;2, 2000.

. Lee S. C, A. Christen, A. T. Black, M. S. Johnson, R. S. Jassal, R. Ketler, Z. Nesic, and M. Merkens: Annual greenhouse gas budget for a bog ecosystem undergoing restoration by rewetting, 2799, https://doi.org/10.5194/bg-14-2799-2017, 2017.

Schulz, C., Martín Brañas, M., Núñez Pérez, C., Del Aguila Villacorta, M., Laurie, N., Lawson, I. T., and Roucoux, K. H.: Uses, cultural significance, and management of peatlands in the

Peruvian Amazon: Implications for conservation, Biological Conservation, 235, 189–198, https://doi.org/10.1016/j.biocon.2019.04.005, 2019.

Silvola, J., Alm, J., Ahlholm, U., Nykanen, H., and Martikainen, P. J.: CO2 Fluxes from Peat in Boreal Mires under Varying Temperature and Moisture Conditions, 84, 219–228, https://doi.org/10.2307/2261357, 1996.

Strack, M. and Waddington, J. M.: Effects of peat extraction and restoration on greenhouse gas exchange from Canadian peatlands, 2012.

Strack, M. and Zuback, Y. C. A.: Annual carbon balance of a peatland 10 yr following restoration, 10, 2885–2896, https://doi.org/10.5194/bg-10-2885-2013, 2013.

Strack, M., Kellner, E., and Waddington, J. M.: Effect of entrapped gas on peatland surface level fluctuations, 20, 3611–3622, https://doi.org/10.1002/hyp.6518, 2006.

Straková, P., Anttila, J., Spetz, P., Kitunen, V., Tapanila, T., and Laiho, R.: Litter quality and its response to water level drawdown in boreal peatlands at plant species and community level, 335, 501–520, https://doi.org/10.1007/s11104-010-0447-6, 2010.

Strilesky, S. L. and Humphreys, E. R.: A comparison of the net ecosystem exchange of carbon dioxide and evapotranspiration for treed and open portions of a temperate peatland, Agricultural and Forest Meteorology, 153, 45–53, https://doi.org/10.1016/j.agrformet.2011.06.006, 2012.

Taillardat, P., Thompson, B. S., Garneau, M., Trottier, K., and Friess, D. A.: Climate change mitigation potential of wetlands and the cost-effectiveness of their restoration, Interface Focus, 10, 20190129, https://doi.org/10.1098/rsfs.2019.0129, 2020.

Tan, L., Ge, Z., Zhou, X., Li, S., Li, X., and Tang, J.: Conversion of coastal wetlands, riparian wetlands and peatlands increases greenhouse gas emissions: A global meta-analysis, https://doi.org/10.1111/gcb.14933, 2019.

Thorslund, J., Jarsjo, J., Jaramillo, F., Jawitz, J. W., Manzoni, S., Basu, N. B., Chalov, S. R., Cohen, M. J., Creed, I. F., Goldenberg, R., Hylin, A., Kalantari, Z., Koussis, A. D., Lyon, S. W., Mazi, K., Mard, J., Persson, K., Pietro, J., Prieto, C., Quin, A., Van Meter, K., and Destouni, G.: Wetlands as large-scale nature-based solutions: Status and challenges for research, engineering and management, Ecological Engineering, 108, 489–497, https://doi.org/10.1016/j.ecoleng.2017.07.012, 2017.

Tiemeyer, B., Freibauer, A., Borraz, E. A., Augustin, J., Bechtold, M., Beetz, S., Beyer, C., Ebli, M., Eickenscheidt, T., Fiedler, S., Förster, C., Gensior, A., Giebels, M., Glatzel, S., Heinichen, J., Hoffmann, M., Höper, H., Jurasinski, G., Laggner, A., Leiber-Sauheitl, K., Peichl-Brak, M., and Drösler, M.: A new methodology for organic soils in national greenhouse gas inventories: Data synthesis, derivation and application, 109, 105838, https://doi.org/10.1016/j.ecolind.2019.105838, 2020.

Tuittila, E.-S., Komulainen, V.-M., Vasander, H., and Laine, J.: Restored cut-away peatland as a sink for atmospheric CO2, Oecologia, 120, 563–574, https://doi.org/10.1007/s004420050891, 1999.

Turetsky, M. R., Treat, C. C., Waldrop, M. P., Waddington, J. M., Harden, J. W., and McGuire, A. D.: Short-term response of methane fluxes and methanogen activity to water table and soil warming manipulations in an Alaskan peatland, 113, https://doi.org/10.1029/2007JG000496, 2008.

Turetsky, M. R., Kotowska, A., Bubier, J., Dise, N. B., Crill, P., Hornibrook, E. R. C., Minkkinen, K., Moore, T. R., Myers-Smith, I. H., Nykänen, H., Olefeldt, D., Rinne, J., Saarnio, S., Shurpali, N., Tuittila, E.-S., Waddington, J. M., White, J. R., Wickland, K. P., and Wilmking, M.: A

synthesis of methane emissions from 71 northern, temperate, and subtropical wetlands, 20, 2183–2197, https://doi.org/10.1111/gcb.12580, 2014.

Vanselow-Algan, M., Schmidt, S. R., Greven, M., Fiencke, C., Kutzbach, L., and Pfeiffer, E. M.: High methane emissions dominated annual greenhouse gas balances 30 years after bog rewetting, 12, 4361–4371, https://doi.org/10.5194/bg-12-4361-2015, 2015.

Waddington, J. M. and Day, S. M.: Methane emissions from a peatland following restoration, 112, n/a-n/a, https://doi.org/10.1029/2007jg000400, 2007.

Waddington, J. M., Strack, M., and Greenwood, M. J.: Toward restoring the net carbon sink function of degraded peatlands: Short-term response in CO2exchange to ecosystem-scale restoration, 115, https://doi.org/10.1029/2009jg001090, 2010.

Walker, A. P., De Kauwe, M. G., Bastos, A., Belmecheri, S., Georgiou, K., Keeling, R. F., McMahon, S. M., Medlyn, B. E., Moore, D. J. P., Norby, R. J., Zaehle, S., Anderson-Teixeira, K. J., Battipaglia, G., Brienen, R. J. W., Cabugao, K. G., Cailleret, M., Campbell, E., Canadell, J. G., Ciais, P., Craig, M. E., Ellsworth, D. S., Farquhar, G. D., Fatichi, S., Fisher, J. B., Frank, D. C., Graven, H., Gu, L., Haverd, V., Heilman, K., Heimann, M., Hungate, B. A., Iversen, C. M., Joos, F., Jiang, M., Keenan, T. F., Knauer, J., Körner, C., Leshyk, V. O., Leuzinger, S., Liu, Y., MacBean, N., Malhi, Y., McVicar, T. R., Penuelas, J., Pongratz, J., Powell, A. S., Riutta, T., Sabot, M. E. B., Schleucher, J., Sitch, S., Smith, W. K., Sulman, B., Taylor, B., Terrer, C., Torn, M. S., Treseder, K. K., Trugman, A. T., Trumbore, S. E., van Mantgem, P. J., Voelker, S. L.,Whelan, M. E., and Zuidema, P. A.: Integrating the evidence for a terrestrial carbon sink caused by increasing atmospheric CO2, New Phytologist, n/a, https://doi.org/10.1111/nph.16866, 2020.

Whalen, S. C.: Methane Oxidation, Production, and Emission at Contrasting Sites in a Boreal Bog, 17, 237–251, https://doi.org/10.1080/01490450050121198, 2010.

Whiting, G. J. and Chanton, J. P.: Plant-dependent CH4 emission in a subarctic Canadian fen, 6, 225–231, https://doi.org/10.1029/92GB00710, 1992.

Wilson, D., Alm, J., Laine, J., Byrne, K. A., Farrell, E. P., and Tuittila, E.-S.: Rewetting of Cutaway Peatlands: Are We Re-Creating Hot Spots of Methane Emissions?, RESTORATION ECOLOGY, 17, 796–806, https://doi.org/10.1111/j.1526-100X.2008.00416.x, 2009.

Wilson, D., Farrell Catherine, A., Fallon, D., Moser, G., Müller, C., and Renou-Wilson, F.: Multiyear greenhouse gas balances at a rewetted temperate peatland, 22, 4080–4095, https://doi.org/10.1111/gcb.13325, 2016a.

Wilson, D., Farrell, C. A., Fallon, D., Moser, G., Muller, C., and Renou-Wilson, F.: Multiyear greenhouse gas balances at a rewetted temperate peatland, 22, 4080–4095, https://doi.org/10.1111/gcb.13325, 2016b.

Wutzler, T., Lucas-Moffat, A., Migliavacca, M., Knauer, J., Sickel, K., Šigut, L., Menzer, O., and Reichstein, M.: Basic and extensible post-processing of eddy covariance flux data with REddyProc, Biogeosciences, 15, 5015–5030, https://doi.org/10.5194/bg-15-5015-2018, 2018.

Yu, L., Huang, Y., Sun, F., and Sun, W.: A synthesis of soil carbon and nitrogen recovery after wetland restoration and creation in the United States, 7, 7966, https://doi.org/10.1038/s41598-017-08511-y, 2017.

Zhao, J., Malo dene, S. L., Oberbauer, S. F., Olivas, P. C., Schedlbauer, J. L., Staudhammer, C. L., and Starr, G.: Intensified inundation shifts a freshwater wetland from a CO2 sink to a source, https://doi.org/10.1111/gcb.14718, 2019.

Zhu, D., Wu, N., Bhattarai, N., Oli, K. P., Chen, H., Rawat, G. S., Rashid, I., Dhakal, M., Joshi, S., Tian, J., Zhu, Q., Chaudhary, S., and Tshering, K.: Methane emissions respond to soil temperature in convergent patterns but divergent sensitivities across wetlands along altitude, https://doi.org/10.1111/gcb.15454, 2020.